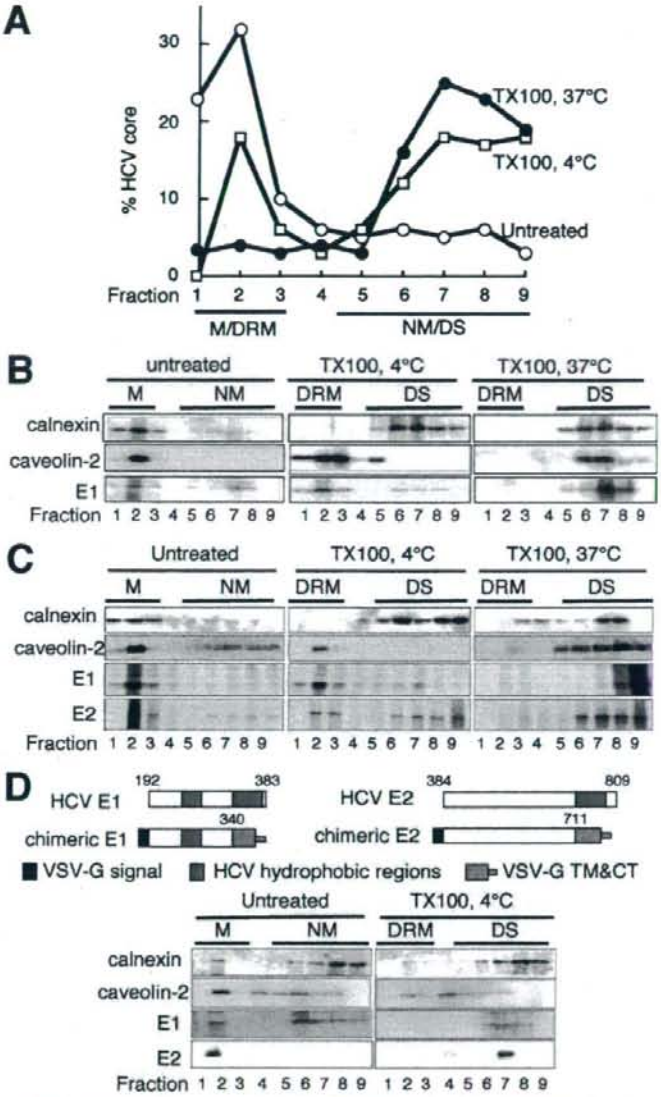

FIG. 4. Compartmentation of HCV structural proteins within DRM fractions. Lysates of HCVcc-infected cells were either treated with 1% TX-100, either on ice or at 37°C, or left untreated, followed by sucrose gradient centrifugation. (A and B) For each fraction, the amount of core protein was determined by an enzyme-linked immunosorbent assay (A), and E1, calnexin, and caveolin-2 were analyzed by Western blotting (B). The amount of core protein in each lysate (TX-100, 37°C; TX-100, 4°C; Untreated) was assigned the arbitrary value of 100%. M, membrane; NM, nonmembrane; DS, detergent soluble. (C) Lysates of 293T cells expressing HCV E1 or E2 protein were either treated with 1% TX-100, either on ice or at 37°C, or left untreated, followed by discontinuous sucrose gradient centrifugation. Each fraction was concentrated in a Centricon YM-30 filter unit and subjected to 12.5% sodium dodecyl sulfate-polyacrylamide gel electrophoresis, followed by immunoblotting with antibodies against calnexin, caveolin-2, Myc (E1), or FLAG (E2). (D) (Top) Structures of HCV envelope genes used. Amino acid positions of HCV are indicated. Signal sequence, transmembrane (TM), and cytoplasmic tail (CT) domains of VSV G protein are shown. (Bottom) Cell lysates expressing chimeric HCV E1 or E2 protein were treated with 1% TX-100 on ice or left untreated, followed by discontinuous sucrose gradient centrifugation. It has been reported that VSV-G is not associated with lipid (39). Calnexin, caveolin-2, and chimeric glycoproteins (chimeric E1 and chimeric E2) were analyzed by immunoblotting. Fractions are numbered from 1 to 9 in order from top to bottom (light to heavy).

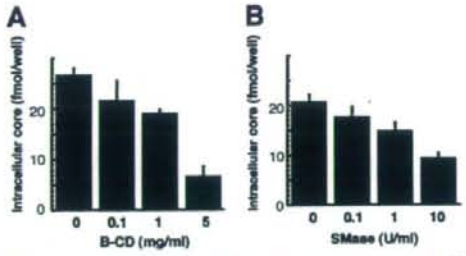

FIG. 5. Effects of B-CD or SMase treatment of cells on HCV infectivity. Huh-7 cells were either left untreated or treated with B-CD at 0.1, 1, or 5 mg/ml (A) or with SMase at 0.1, 1, or 10 U/ml (B) prior to HCVcc infection. Intracellular core levels were quantitated 72 h p.i. Data are means from four independent experiments. Error bars, standard deviations.

proteins are important for their interaction (Fig. 4D). These data suggest that subpopulations of HCV structural proteins are associated with lipid rafts in cells generating the HCV particles.

Moderate inhibition of HCV infection by B-CD or SMase treatment of host cells. It has recently been reported that cholesterol depletion or SM hydrolysis from the host cell membrane decreases HCV infection, in part by decreasing the level of CD81 on the cell surface (19, 53). The involvement of the lipid environment of the host cell plasma membrane in HCV infection was investigated in our HCVcc infection system. Prior to infection, Huh-7 cells were treated with B-CD or SMase and then washed with the medium five times. Cholesterol depletion from Huh-7 cells by B-CD at 1 or 5 mg/ml inhibited HCV core levels by 20 and 75%, respectively, compared to levels in untreated cells (Fig. 5A). We also found that hydrolysis of SM by SMase at 1 or 10 U/ml on the cells, respectively, led to moderate reduction of the viral infection, by 20 or 55% of the infection level of the untreated control (Fig. 5B). There was no influence on cell viability under the conditions of these treatments (data not shown). These findings, compared with the results in Fig. 1A and 2A, suggest that the raft-like environment on the plasma membrane likely serves as a portal for HCV entry, but HCV virion-associated cholesterol and sphingolipid more readily play more critical roles in viral infection.

Inhibitors of the sphingolipid biosynthetic pathway suppress the production of HCVcc, but not RNA replication, for a JFH-1-derived replicon. In the course of studying the involvement of lipid metabolism in the HCV life cycle, we observed that inhibitors of the sphingolipid biosynthetic pathway, including ISP-1 and HPA-12, which specifically inhibit serine palmitoyltransferase (31) and ceramide trafficking from the ER to the Golgi apparatus (55), influenced subgenomic replicons derived from the HCV-N isolate (genotype 1b), but not those derived from JFH-1. A dose-dependent decrease in HCV RNA copy numbers among HCV-N replicon cells was observed upon exposure to ISP-1 or HPA-12, as previously reported (43, 52). In contrast, these compounds had little or no effect on viral RNA accumulation in JFH-1 replicon cells (Fig. 6A). Furthermore, these compounds did not affect luciferase activity in the lysates of Huh-7 cells transfected with an in vitro-transcribed JFH-1 replicon RNA containing a luciferase reporter gene (22) (data not shown). Figure 6B shows the effects of ISP-1 and HPA-12 on de novo sphingolipid biosynthesis by replicon cells. No differences in the inhibitory effects of each compound were observed in replicon cells derived from HCV-N versus JFH-1. When de novo synthesis of sphingolipids was examined by metabolic labeling with [^{14}C]serine, ISP-1 almost completely inhibited the production of both ceramide and SM, while HPA-12 greatly inhibited the synthesis of SM but not ceramide. Levels of phosphatidylethanolamine and phosphatidylserine, into which serine is incorporated by a pathway distinct from that of sphingolipid biosynthesis, were not influenced by these drugs. These results suggest that suppression of HCV RNA replication by inhibitors of sphingolipid biosynthesis might be dependent on the viral genotype or isolate.

This observation prompted us to investigate whether inhibitors of the sphingolipid biosynthetic pathway might have the ability to prevent HCV virion production. Interestingly, when Huh-7 cells producing JFH-1 HCVcc were treated with ISP-1 or HPA-12 under conditions similar to those the replicon cells, viral core levels in the culture supernatants were greatly reduced in a dose-dependent manner. For example, exposure to 10 μM ISP-1 or 1 μM HPA-12 reduced viral core protein levels more than 85% from those for control cells (Fig. 6C). The 50% inhibitory concentrations of both drugs were less than 0.1 μM, 50-fold less than those obtained for the RNA replication of the HCV-N-replicon. Together, these results suggest that the sphingolipid biosynthetic pathway plays an important role in the production of HCV particles, but not in genome replication, in JFH-1-based HCVcc.

DISCUSSION

In this study, we demonstrated the role of HCV virion-associated cholesterol and sphingolipid in viral infectivity. Although dependence on virion-associated cholesterol for virus entry has been shown for a number of viruses (4, 6, 28, 49), this is the first study to demonstrate the importance of envelope cholesterol in a virus belonging to the family *Flaviviridae*. Furthermore, to our knowledge, the functional role of virion membrane-associated SM has not been examined in viruses. Our previous studies using Chinese hamster ovary cell mutants deficient in SM synthesis have demonstrated that reduction of cellular SM levels enhances cellular cholesterol efflux in the presence of B-CD (9, 12). Thus, it may be possible that SM plays a role in the retention of cholesterol on HCV particles due to interaction between cholesterol and SM. The finding that B-CD or SMase treatment of HCVcc markedly inhibited virus internalization but not cell attachment (Fig. 3) suggests that HCV membrane-associated cholesterol and sphingolipid are crucial for the interaction of viral glycoproteins with the virus-receptor/coreceptor required for cell entry. Cholesterol depletion or sphingolipid hydrolysis might induce a conformational change in the viral envelope, resulting in instability of the virion structure. Since the cholesterol/phospholipid ratios of membranes affect bilayer fluidity, the maturation of viral envelopes with high cholesterol/phospholipid ratios via association with rafts may be important for the stability of HCV

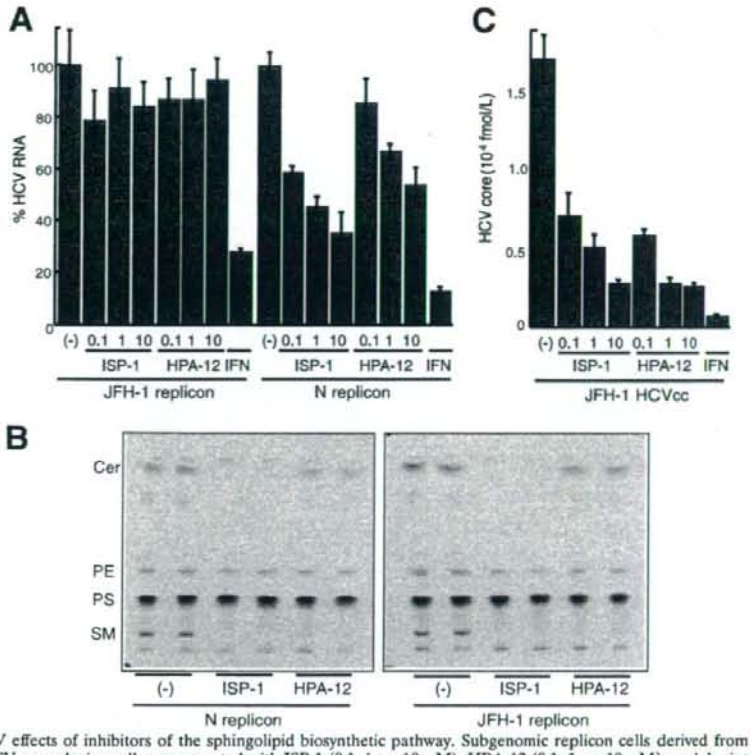

FIG. 6. Anti-HCV effects of inhibitors of the sphingolipid biosynthetic pathway. Subgenomic replicon cells derived from HCV isolate N or JFH-1, as well as HCVcc-producing cells, were treated with ISP-1 (0.1, 1, or 10 μM), HPA-12 (0.1, 1, or 10 μM) or alpha interferon (IFN) (100 U/ml) for 72 h. HCV RNA titers in the replicon cells (A) and the HCV core protein content of the culture medium of infected cells (C) were determined. Data are means from four independent experiments. Error bars, standard deviations. (B) De novo synthesis of sphingolipid in the absence or presence of ISP-1 (10 μM) and HPA-12 (10 μM) was monitored in duplicate by metabolic labeling with [^{14}C]serine for 2 h at 37°C. Cer, ceramide; PE, phosphatidylethanolamine; PS, phosphatidylserine.

particles. Replenishing the viral membrane with cholesterol following treatment with 5 mg/ml B-CD successfully restored viral infectivity to the same level as that of untreated virus (Fig. 1), suggesting that reversible B-CD-induced changes in HCV structure might critically influence viral infectivity. However, we were unable to restore viral infectivity by replenishing cholesterol after pretreatment of the virion with concentrations of B-CD exceeding 10 mg/ml (data not shown). Under these conditions, it is likely that large holes in the viral membrane destroy the virus, a result that cannot be reversed by supplying exogenous cholesterol.

How are cholesterol and sphingolipid involved in the HCV virion during the process of virus maturation? Like most positive-stranded RNA viruses, HCV is thought to assemble at the ER membrane. However, Miyanari et al. (32) reported that lipid droplets are important for HCVcc formation. These authors have shown that the characteristics of lipid-droplet-associated membranes in Huh-7 cells differ from those of ER membranes. In the case of flaviviruses, for which the mechanism of viral assembly and budding remains unclear (15), a few studies have demonstrated budding at the plasma membrane (13, 36, 37, 41), and it has been proposed that the site of budding may be virus and cell type dependent (27). We demonstrate here that subpopulations of HCV structural proteins partition into cellular detergent-resistant, lipid-raft-like membrane fractions in HCVcc-producing cells (Fig. 4) and that inhibitors of the sphingolipid biosynthetic pathway block HCV virion production (Fig. 6). Furthermore, a large proportion of HCV E2 protein incorporated into HCVcc is endoglycosidase H resistant (data not shown). Thus, membrane compartments containing cholesterol- and sphingolipid-rich microdomains may be involved in HCV virion maturation. Another explanation for the recruitment of these lipids to the HCV membrane may be an association between the virus and very-low-density lipoprotein (VLDL) or low-density lipoprotein. Recently, Huang et al. (16) demonstrated a close link between HCV production and VLDL assembly, suggesting that an HCV-VLDL complex is generated and secreted from cells.

Recent reports have demonstrated that CD81-mediated HCV infection is partly dependent on cell membrane choles-

terol (19) and SM (53). We further characterized the role of lipid on the plasma membrane in viral infectivity and found that cholesterol depletion by B-CD, as well as hydrolysis of SM by SMase, moderately inhibits HCV infectivity (Fig. 5). These results suggest that cholesterol and sphingolipid in the plasma membrane environment may assist HCV entry, while HCV virion-associated cholesterol and sphingolipid appear to play critical roles in viral infection.

We previously demonstrated that HCV RNA and nonstructural proteins are present in DRM structures, likely in the context of a lipid-raft structure, and that viral RNA is likely synthesized at a raft membrane structure in cells containing the genotype 1b HCV replicon (2, 10, 46). Here we observed that ISP-1 and HPA-12 suppress HCVcc production, but not viral RNA replication, by the JFH-1 replicon (Fig. 6). Impairment of particle assembly and maturation, rather than suppression of genome replication, by these drugs may account for the inhibition of HCV production in the JFH-1 system. Viral RNA replication of the HCV-N replicon, however, was efficiently inhibited by these compounds, as found in previous reports (43). The virus strain specificity of the anti-HCV activity of cyclosporine has recently been demonstrated: JFH-1 replication is less sensitive to cyclosporine than replication of genotype 1b strains. Furthermore, the requirement for interaction with a cellular replication cofactor, cyclophilin B, differs among HCV strains (18). It appears that ISP-1 and HPA-12 are further examples of diverse effects on HCV strain replication.

In summary, our data here demonstrate important roles of cholesterol and sphingolipid in HCV infection and virion maturation. Specifically, mature HCV particles are rich in cholesterol. Depletion from HCV or hydrolysis of virion-associated SM results in a loss of infectivity. Moreover, the addition of exogenous cholesterol restores infectivity. In addition, cholesterol and sphingolipid on the HCV membrane play key roles in virus internalization, and portions of structural proteins are localized at lipid-raft-like membrane structures within cells. Finally, inhibitors of the sphingolipid biosynthetic pathway efficiently block virion production. These observations suggest that agents capable of modifying virion-associated lipid content might function as antivirals by preventing and/or blocking HCV infection and production.

ACKNOWLEDGMENTS

We thank M. Matsuda, M. Sasaki, S. Yoshizaki, T. Shimoji, M. Kaga, and T. Date for technical assistance and T. Mizoguchi for secretarial work.

This work was partially supported by a grant-in-aid for Scientific Research from the Japan Society for the Promotion of Science, from the Ministry of Health, Labor, and Welfare of Japan, and from the Ministry of Education, Culture, Sports, Science, and Technology, as well as by a Research on Health Science Focusing on Drug Innovation grant from the Japan Health Sciences Foundation.

REFERENCES

1. **Aizaki, H., Y. Aoki, T. Harada, K. Ishii, T. Suzuki, S. Nagamori, G. Toda, Y. Matsuura, and T. Miyamura.** 1998. Full-length complementary DNA of hepatitis C virus genome from an infectious blood sample. Hepatology **27:** 621–627.
2. **Aizaki, H., K. J. Lee, V. M. Sung, H. Ishiko, and M. M. Lai.** 2004. Characterization of the hepatitis C virus RNA replication complex associated with lipid rafts. Virology **324:**450–461.
3. **Akazawa, D., T. Date, K. Morikawa, A. Murayama, M. Miyamoto, M. Kaga, H. Barth, T. F. Baumert, J. Dubuisson, and T. Wakita.** 2007. CD81 expression is important for the permissiveness of Huh7 cell clones for heterogeneous hepatitis C virus infection. J. Virol. **81:**5036–5045.
4. **Bender, F. C., J. C. Whitbeck, H. Lou, G. H. Cohen, and R. J. Eisenberg.** 2005. Herpes simplex virus glycoprotein B binds to cell surfaces independently of heparan sulfate and blocks virus entry. J. Virol. **79:**11588–11597.
5. **Blanchard, E., D. Brand, S. Trassard, A. Goudeau, and P. Roingeard.** 2002. Hepatitis C virus-like particle morphogenesis. J. Virol. **76:**4073–4079.
6. **Chazal, N., and D. Gerlier.** 2003. Virus entry, assembly, budding, and membrane rafts. Microbiol. Mol. Biol. Rev. **67:**226–237.
7. **Evans, M. J., T. von Hahn, D. M. Tscherne, A. J. Syder, M. Panis, B. Wolk, T. Hatziioannou, J. A. McKeating, P. D. Bieniasz, and C. M. Rice.** 2007. Claudin-1 is a hepatitis C virus co-receptor required for a late step in entry. Nature **446:**801–805.
8. **Ezelle, H. J., D. Markovic, and G. N. Barber.** 2002. Generation of hepatitis C virus-like particles by use of a recombinant vesicular stomatitis virus vector. J. Virol. **76:**12325–12334.
9. **Fukasawa, M., M. Nishijima, H. Itabe, T. Takano, and K. Hanada.** 2000. Reduction of sphingomyelin level without accumulation of ceramide in Chinese hamster ovary cells affects detergent-resistant membrane domains and enhances cellular cholesterol efflux to methyl-β-cyclodextrin. J. Biol. Chem. **275:**34028–34034.
10. **Gao, L., H. Aizaki, J. W. He, and M. M. Lai.** 2004. Interactions between viral nonstructural proteins and host protein hVAP-33 mediate the formation of hepatitis C virus RNA replication complex on lipid raft. J. Virol. **78:**3480–3488.
11. **Guo, J. T., V. V. Bichko, and C. Seeger.** 2001. Effect of alpha interferon on the hepatitis C virus replicon. J. Virol. **75:**8516–8523.
12. **Hanada, K., T. Hara, M. Fukasawa, A. Yamaji, M. Umeda, and M. Nishijima.** 1998. Mammalian cell mutants resistant to a sphingomyelin-directed cytolysin. Genetic and biochemical evidence for complex formation of the LCB1 protein with the LCB2 protein for serine palmitoyltransferase. J. Biol. Chem. **273:**33787–33794.
13. **Hase, T., P. L. Summers, K. H. Eckels, and W. B. Baze.** 1987. An electron and immunoelectron microscopic study of dengue-2 virus infection of cultured mosquito cells: maturation events. Arch. Virol. **92:**273–291.
14. **Heider, J. G., and R. L. Boyett.** 1978. The picomole determination of free and total cholesterol in cells in culture. J. Lipid Res. **19:**514–518.
15. **Heinz, F. X., and S. L. Allison.** 2003. Flavivirus structure and membrane fusion. Adv. Virus Res. **59:**63–97.
16. **Huang, H., F. Sun, D. M. Owen, W. Li, Y. Chen, M. Gale, and J. Ye.** 2007. Hepatitis C virus production by human hepatocytes dependent on assembly and secretion of very low-density lipoproteins. Proc. Natl. Acad. Sci. USA **104:**5848–5853.
17. **Ikeda, M., M. Yi, K. Li, and S. M. Lemon.** 2002. Selectable subgenomic and genome-length dicistronic RNAs derived from an infectious molecular clone of the HCV-N strain of hepatitis C virus replicate efficiently in cultured Huh7 cells. J. Virol. **76:**2997–3006.
18. **Ishii, N., K. Watashi, T. Hishiki, K. Goto, D. Inoue, M. Hijikata, T. Wakita, N. Kato, and K. Shimotohno.** 2006. Diverse effects of cyclosporine on hepatitis C virus strain replication. J. Virol. **80:**4510–4520.
19. **Kapadia, S. B., H. Barth, T. Baumert, J. A. McKeating, and F. V. Chisari.** 2007. Initiation of hepatitis C virus infection is dependent on cholesterol and cooperativity between CD81 and scavenger receptor B type I. J. Virol. **81:**374–383.
20. **Kato, T., A. Furusaka, M. Miyamoto, T. Date, K. Yasui, J. Hiramoto, K. Nagayama, T. Tanaka, and T. Wakita.** 2001. Sequence analysis of hepatitis C virus isolated from a fulminant hepatitis patient. J. Med. Virol. **64:**334–339.
21. **Kato, T., T. Date, M. Miyamoto, A. Furusaka, K. Tokushige, M. Mizokami, and T. Wakita.** 2003. Efficient replication of the genotype 2a hepatitis C virus subgenomic replicon. Gastroenterology **125:**1808–1817.
22. **Kato, T., T. Date, M. Miyamoto, M. Sugiyama, Y. Tanaka, E. Orito, T. Ohno, K. Sugihara, I. Hasegawa, K. Fujiwara, K. Ito, A. Ozasa, M. Mizokami, and T. Wakita.** 2005. Detection of anti-hepatitis C virus effects of interferon and ribavirin by a sensitive replicon system. J. Clin. Microbiol. **43:**5679–5684.
23. **Kato, T., T. Date, A. Murayama, K. Morikawa, D. Akazawa, and T. Wakita.** 2006. Cell culture and infection system for hepatitis C virus. Nat. Protoc. **1:**2334–2339.
24. **Kobayashi, S., K. Kakumoto, and M. Sugiura.** 2002. Transition metal salts-catalyzed aza-Michael reactions of enones with carbamates. Org. Lett. **18:** 1319–1322.
25. **Koutsoudakis, G., E. Herrmann, S. Kallis, R. Bartenschlager, and T. Pietschmann.** 2007. The level of CD81 cell surface expression is a key determinant for productive entry of hepatitis C virus into host cells. J. Virol. **81:**588–598.
26. **Lohmann, V., F. Korner, J. Koch, U. Herian, L. Theilmann, and R. Bartenschlager.** 1999. Replication of subgenomic hepatitis C virus RNAs in a hepatoma cell line. Science **285:**110–113.
27. **Mackenzie, J. M., and E. G. Westaway.** 2001. Assembly and maturation of the flavivirus Kunjin virus appear to occur in the rough endoplasmic reticulum and along the secretory pathway, respectively. J. Virol. **75:**10787–10799.
28. **Manes, S., G. del Real, R. A. Lacalle, P. Lucas, C. Gomez-Mouton, S. Sanchez-Palomino, R. Delgado, J. Alcami, E. Mira, and A. C. Martinez.**

2000. Membrane raft microdomains mediate lateral assemblies required for HIV-1 infection. EMBO 1:190–196.
29. **Matsuo, E., H. Tani, C. Lim, Y. Komoda, T. Okamoto, H. Miyamoto, K. Moriishi, S. Yagi, A. H. Patel, T. Miyamura, and Y. Matsuura.** 2006. Characterization of HCV-like particles produced in a human hepatoma cell line by a recombinant baculovirus. Biochem. Biophys. Res. Commun. **340**:200–208.
30. **Matto, M., C. M. Rice, B. Aroeti, and J. S. Glenn.** 2004. Hepatitis C virus core protein associates with detergent-resistant membranes distinct from classical plasma membrane rafts. J. Virol. **78**:12047–12053.
31. **Miyake, Y., Y. Kozutsumi, S. Nakamura, T. Fujita, and T. Kawasaki.** 1995. Serine palmitoyltransferase is the primary target of a sphingosine-like immunosuppressant, ISP-1/myriocin. Biochem. Biophys. Res. Commun. **211**: 396–403.
32. **Miyanari, Y., K. Atsuzawa, N. Usuda, K. Watashi, T. Hishiki, M. Zayas, R. Bartenschlager, T. Wakita, M. Hijikata, and K. Shimotohno.** 2007. The lipid droplet is an important organelle for hepatitis C virus production. Nat. Cell Biol. **9**:1089–1097.
33. **Morikawa, K., Z. Zhao, T. Date, M. Miyamoto, A. Murayama, D. Akazawa, J. Tanabe, S. Sone, and T. Wakita.** 2007. The roles of CD81 and glycosaminoglycans in the adsorption and uptake of infectious HCV particles. J. Med. Virol. **79**:714–723.
34. **Murakami, K., K. Ishii, Y. Ishihara, S. Yoshizaki, K. Tanaka, Y. Gotoh, H. Aizaki, M. Kohara, H. Yoshioka, Y. Mori, N. Manabe, I. Shoji, T. Sata, R. Bartenschlager, Y. Matsuura, T. Miyamura, and T. Suzuki.** 2006. Production of infectious hepatitis C virus particles in three-dimensional cultures of the cell line carrying the genome-length dicistronic viral RNA of genotype 1b. Virology **351**:381–392.
35. **Nakai, K., T. Okamoto, T. Kimura-Someya, K. Ishii, C. K. Lim, H. Tani, E. Matsuo, T. Abe, Y. Mori, T. Suzuki, T. Miyamura, J. H. Nunberg, K. Moriishi, and Y. Matsuura.** 2006. Oligomerization of hepatitis C virus core protein is crucial for interaction with the cytoplasmic domain of E1 envelope protein. J. Virol. **80**:11265–11273.
36. **Ng, M. L., J. Howe, V. Sreenivasan, and J. J. Mulders.** 1994. Flavivirus West Nile (Sarafend) egress at the plasma membrane. Arch. Virol. **137**:303–313.
37. **Ng, M. L., S. H. Tan, and J. J. Chu.** 2001. Transport and budding at two distinct sites of visible nucleocapsids of West Nile (Sarafend) virus. J. Med. Virol. **65**:758–764.
38. **Niwa, H., K. Yamamura, and J. Miyazaki.** 1991. Efficient selection for high-expression transfectants with a novel eukaryotic vector. Gene **108**:193–199.
39. **Pessin, J. E., and M. Glaser.** 1980. Budding of Rous sarcoma virus and vesicular stomatitis virus from localized lipid regions in the plasma membrane of chicken embryo fibroblasts. J. Biol. Chem. **255**:9044–9050.
40. **Pitha, J., T. Irie, P. B. Sklar, and J. S. Nye.** 1988. Drug solubilizers to aid pharmacologists: amorphous cyclodextrin derivatives. Life Sci. **43**:493–502.
41. **Rahman, S., T. Matsumura, K. Masuda, K. Kanemura, and T. Fukunaga.** 1998. Maturation site of dengue type 2 virus in cultured mosquito C6/36 cells and Vero cells. Kobe J. Med. Sci. **44**:65–79.
42. **Rouser, G., G. Galli, and G. Kritchevsky.** 1967. Lipid composition of the normal human brain and its variations during various diseases. Pathol. Biol. **15**:195–200.
43. **Sakamoto, H., K. Okamoto, M. Aoki, H. Kato, A. Katsume, A. Ohta, T. Tsukuda, N. Shimma, Y. Aoki, M. Arisawa, M. Kohara, and M. Sudoh.** 2005. Host sphingolipid biosynthesis as a target for hepatitis C virus therapy. Nat. Chem. Biol. **1**:333–337.
44. **Sato, K., H. Okamoto, S. Aihara, Y. Hoshi, T. Tanaka, and S. Mishiro.** 1993. Demonstration of sugar moiety on the surface of hepatitis C virions recovered from the circulation of infected humans. Virology **196**:354–357.
45. **Serafino, A., M. B. Valli, F. Andreola, A. Crema, G. Ravagnan, L. Bertolini, and G. Carloni.** 2003. Suggested role of the Golgi apparatus and endoplasmic reticulum for crucial sites of hepatitis C virus replication in human lymphoblastoid cells infected in vitro. J. Med. Virol. **70**:31–41.
46. **Shi, S. T., K. J. Lee, H. Aizaki, S. B. Hwang, and M. M. Lai.** 2003. Hepatitis C virus RNA replication occurs on a detergent-resistant membrane that cofractionates with caveolin-2. J. Virol. **77**:4160–4168.
47. **Shinitzky, M., and M. Inbar.** 1976. Microviscosity parameters and protein mobility in biological membranes. Biochim. Biophys. Acta **433**:133–149.
48. **Shirakura, M., K. Murakami, T. Ichimura, R. Suzuki, T. Shimoji, K. Fukuda, K. Abe, S. Sato, M. Fukasawa, Y. Yamakawa, M. Nishijima, K. Moriishi, Y. Matsuura, T. Wakita, T. Suzuki, P. M. Howley, T. Miyamura, and I. Shoji.** 2007. E6AP ubiquitin ligase mediates ubiquitylation and degradation of hepatitis C virus core protein. J. Virol. **81**:1174–1185.
49. **Stuart, A. D., H. E. Eustace, T. A. McKee, and T. D. Brown.** 2002. A novel cell entry pathway for a DAF-using human enterovirus is dependent on lipid rafts. J. Virol. **76**:9307–9322.
50. **Takikawa, S., K. Ishii, H. Aizaki, T. Suzuki, H. Asakura, Y. Matsuura, and T. Miyamura.** 2000. Cell fusion activity of hepatitis C virus envelope proteins. J. Virol. **74**:5066–5074.
51. **Tani, H., Y. Komoda, E. Matsuo, K. Suzuki, I. Hamamoto, T. Yamashita, K. Moriishi, K. Fujiyama, T. Kanto, N. Hayashi, A. Owsianka, A. H. Patel, M. A. Whitt, and Y. Matsuura.** 2007. Replication-competent recombinant vesicular stomatitis virus encoding hepatitis C virus envelope proteins. J. Virol. **81**:8601–8612.
52. **Umehara, T., M. Sudoh, F. Yasui, C. Matsuda, Y. Hayashi, K. Chayama, and M. Kohara.** 2006. Serine palmitoyltransferase inhibitor suppresses HCV replication in a mouse model. Biochem. Biophys. Res. Commun. **346**:67–73.
53. **Voisset, C., M. Lavie, F. Helle, A. Op De Beeck, A. Bilheu, J. Bertrand-Michel, F. Tercé, L. Cocquerel, C. Wychowski, N. Vu-Dac, and J. Dubuisson.** 2008. Ceramide enrichment of the plasma membrane induces CD81 internalization and inhibits hepatitis C virus entry. Cell. Microbiol. **10**:606–617.
54. **Wakita, T., T. Pietschmann, T. Kato, T. Date, M. Miyamoto, Z. Zhao, K. Murthy, A. Habermann, H. G. Krausslich, M. Mizokami, R. Bartenschlager, and T. J. Liang.** 2005. Production of infectious hepatitis C virus in tissue culture from a cloned viral genome. Nat. Med. **11**:791–796.
55. **Yasuda, S., H. Kitagawa, M. Ueno, H. Ishitani, M. Fukasawa, M. Nishijima, S. Kobayashi, and K. Hanada.** 2001. A novel inhibitor of ceramide trafficking from the endoplasmic reticulum to the site of sphingomyelin synthesis. J. Biol. Chem. **276**:43994–44002.
56. **Zhong, J., P. Gastaminza, G. Cheng, S. Kapadia, T. Kato, D. R. Burton, S. F. Wieland, S. L. Uprichard, T. Wakita, and F. V. Chisari.** 2005. Robust hepatitis C virus infection in vitro. Proc. Natl. Acad. Sci. USA **102**:9294–9299.

Virology 383 (2009) 319–327

Contents lists available at ScienceDirect

Virology

journal homepage: www.elsevier.com/locate/yviro

Cellular vimentin content regulates the protein level of hepatitis C virus core protein and the hepatitis C virus production in cultured cells

Yuko Nitahara-Kasahara [a,1], Masayoshi Fukasawa [a,*], Fumiko Shinkai-Ouchi [a], Shigeko Sato [a], Tetsuro Suzuki [b], Kyoko Murakami [b], Takaji Wakita [b], Kentaro Hanada [a], Tatsuo Miyamura [c], Masahiro Nishijima [a,d]

[a] Department of Biochemistry and Cell Biology, National Institute of Infectious Diseases, 1-23-1, Toyama, Shinjuku-ku, Tokyo 162-8640, Japan
[b] Department of Virology II, National Institute of Infectious Diseases, Tokyo 162-8640, Japan
[c] National Institute of Infectious Diseases, Tokyo 162-8640, Japan
[d] National Institute of Health Sciences, Tokyo 158-8501, Japan

ARTICLE INFO

Article history:
Received 14 August 2008
Returned to author for revision
3 September 2008
Accepted 6 October 2008
Available online 14 November 2008

Keywords:
Hepatitis C virus
Core protein
Vimentin

ABSTRACT

Hepatitis C virus (HCV) core protein is essential for virus particle formation. Using HCV core-expressing and non-expressing Huh7 cell lines, Uc39-6 and Uc321, respectively, we performed comparative proteomic studies of proteins in the 0.5% Triton X-100-insoluble fractions of cells, and found that core-expressing Uc39-6 cells had much lower vimentin content than Uc321 cells. In experiments using vimentin-overexpressing and vimentin-knocked-down cells, we demonstrated that core protein levels were affected by cellular vimentin content. When vimentin expression was knocked-down, there was no difference in mRNA level of core protein; but proteasome-dependent degradation of the core protein was strongly reduced. These findings suggest that the turnover rate of core protein is regulated by cellular vimentin content. HCV production was also affected by cellular vimentin content. Our findings together suggest that modulation of hepatic vimentin expression might enable the control of HCV production.

Introduction

Hepatitis C virus (HCV) is a major causative agent of chronic hepatitis (Choo et al., 1989; Kuo et al., 1989). Persistent HCV infection, which develops in at least 70% of infected patients, is strongly correlated with the development of severe liver diseases such as fibrosis, steatosis, cirrhosis, and hepatocellular carcinomas (HCC). Since more than 170 million people in the world are currently infected with HCV (Choo et al., 1989) and there is no treatment completely effective in curing HCV, HCV infection is one of the most important global public health issues. Understanding of the life cycle of HCV and the mechanism by which HCV induces serious liver diseases is crucial for the development of novel anti-HCV strategies.

HCV is an RNA virus of the *Flaviviridae* family and possesses a single-stranded, positive-sense RNA genome of ~9.6 kb (Bartenschlager and Lohmann, 2000). The HCV RNA genome encodes a polyprotein of ~3000 amino acids that is processed by host and viral proteases into 10 individual components including 4 structural and 6 nonstructural proteins (reviewed by Reed and Rice, 2000). HCV core protein is crucial for virus particle production as the structural component of the viral nucleocapsid and as a unit required for formation of the active HCV replication/assembly complex in host cells (Boulant et al., 2007; Miyanari et al., 2007). In addition, the core protein plays pivotal roles in the pathogenesis of HCV infection, as suggested by the finding that transgenic mice expressing core protein in the liver tend to develop liver steatosis with subsequent HCC (Moriya et al., 1998; Moriya et al., 1997). A large number of studies have revealed that a variety of host proteins interact with the core protein (Suzuki et al., 2007). Although these interactions can markedly affect various biological functions in host cells, it is not clearly known yet which interactions and molecules play roles in HCV production or its pathogenicity. Recent exhaustive gene-silencing analyses of host factors using RNAi demonstrated that RNA helicase DDX3, one of the proteins that interacts with the core, is required for HCV RNA replication as well as HCV production (Ariumi et al., 2007; Randall et al., 2007).

In host hepatic cells, HCV core protein is distributed preferentially in the detergent-resistant fractions (Matto et al., 2004), and HCV RNA replication also occurs on detergent-resistant membranes (Aizaki et al., 2004; Shi et al., 2003), suggesting that host factors in the detergent-resistant fractions play roles in core protein functions. In this study, we focused on HCV core protein and the detergent-insoluble proteins of host cells, and performed comparative targeted proteomic analysis of the detergent-insoluble proteins in HCV core-expressing and non-expressing hepatic cells. We identified vimentin as a protein the amount of which was reduced in core-expressing cell lines, and demonstrated that cellular vimentin content affects levels of HCV core protein through the proteasome-mediated protein

* Corresponding author. Fax: +81 3 5285 1157.
E-mail address: fuka@nih.go.jp (M. Fukasawa).
[1] Present address: National Institute of Neuroscience, National Center of Neurology and Psychiatry, Tokyo 187-8502, Japan.

0042-6822/$ – see front matter © 2008 Published by Elsevier Inc.
doi:10.1016/j.virol.2008.10.009

degradation system. Since cellular vimentin levels ultimately affected HCV production, vimentin may be a novel target for strategies of anti-HCV treatment.

Results

Proteomic analysis of detergent-insoluble fractions (DISFs) by second-dimensional polyacrylamide gel electrophoresis (2D-PAGE)/MALDI-QIT-TOF MS

DISFs and detergent-soluble fractions (DSFs) were prepared from HCV core-expressing Uc39-6 and non-expressing Uc321 cells by a sucrose density gradient ultracentrifugation method as described in Materials and methods. Proteins in the DISFs and DSFs were analyzed by immunoblotting with antibodies to HCV core protein and various organelle markers (Fig. 1A). A significant amount of HCV core protein (~70%) was distributed in the DISF of Uc39-6 cells. Nuclear proteins such as laminA/C and laminB were concentrated only in the DISFs of both types of cells, whereas other organelle proteins such as annexin II (plasma membrane), fatty acid synthase (cytosol), prohibitin (mitochondria), and calnexin (endoplasmic reticulum) were detected in the DSFs but not DISFs (Fig. 1A), suggesting that the DISFs in both types of cells contain minor (~15%) discrete populations of cellular proteins. Next, we performed 2D-PAGE analysis of the DISFs in Uc321 and Uc39-6 cells. Proteins in the DISFs were separated by isoelectric focusing (IEF) (pH 4–7) and 12% sodium dodecyl sulfate (SDS)-PAGE, and visualized by SYPRO-Ruby staining (Fig. 1B). Intensity of each spot in 2-D images was compared between Uc321 and Uc39-6 cells. The most difference in DISF proteins between Uc321 and Uc39-6 cells (the Uc39-6/Uc321 ratios of intensity normalized with actin: 10.8–28.0) was detected in the spots numbered as 1 in Fig. 1B (MW ~ 57 kDa, pI ~ 4.7), in which vimentin alone was identified by mass spectrometric analysis. We therefore focused on the relationship between cellular vimentin and core protein in further investigations.

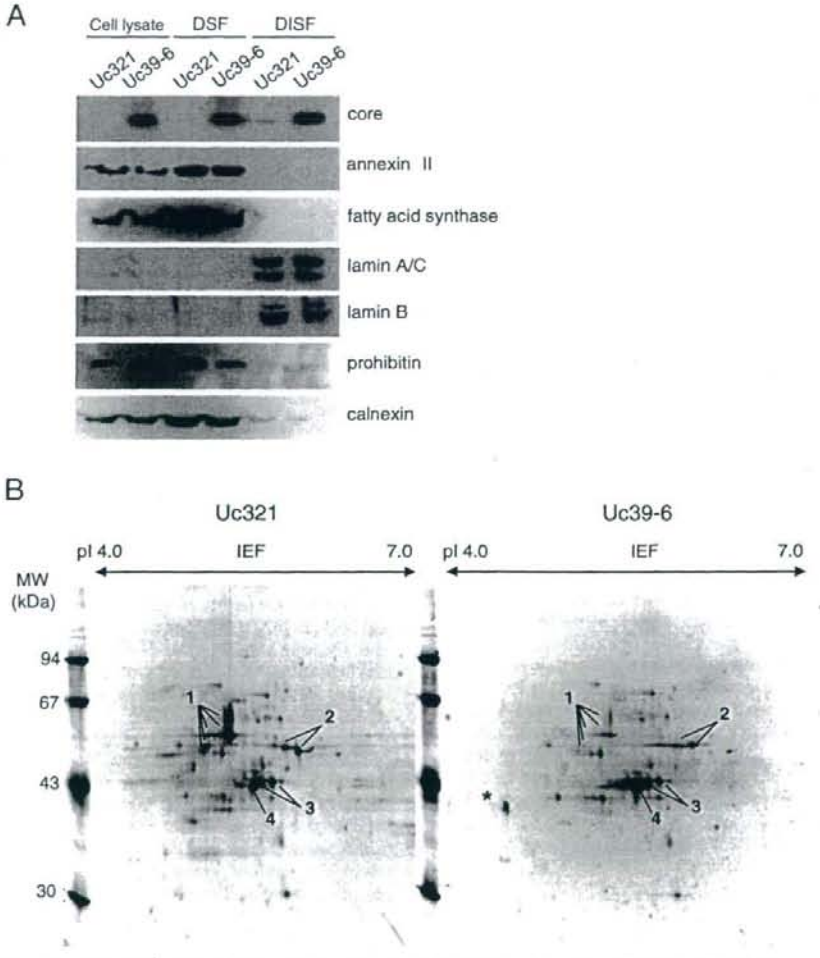

Fig. 1. Immunoblot and 2D-PAGE analysis of DISFs. (A) Total cell lysate fractions (5 μg of protein), DSFs (50 μg of protein), and DISFs (5 μg of protein) from core-expressing Uc39-6 and non-expressing Uc321 cells were analyzed by immunoblotting with antibodies to HCV core protein and various organelle markers as indicated. (B) 2D-PAGE analysis of proteins in DISFs of Uc321 and Uc39-6 cells. Proteins (150 μg) were separated by IEF (pH 4–7), followed by SDS-PAGE on a 12% gel. The gels were stained with SYPRO-Ruby. Major spots, identified as cytoskeletal proteins, are marked: 1, vimentin; 2, cytokeratin 8; 3, cytokeratin 18; 4, actin. *: a non-specific spot.

HCV core-expressing cell lines exhibited reduced vimentin content

To confirm the reduction of vimentin levels in DISFs of HCV core-expressing Uc39-6 cells, immunoblot analysis was performed using anti-vimentin antibody. Uc39-6 cells exhibited lower vimentin contents not only in DISF but also the total cell lysate fraction compared with control Uc321 cells (Fig. 2A). Similar results were obtained in the cell lysate fraction of another independent clone of an HCV core-expressing Huh7 cell line, Uc39-2 (Fig. 2B). Furthermore, a core-expressing hepatic HepG2 cell line, Hep39, also had lower vimentin content than a control cell line, Hepswx (Fig. 2C). These findings exclude the possibility that the reduction of vimentin levels in core-expressing cell lines is a clone- or cell-specific event. Consistent with these findings, levels of vimentin mRNA in Uc39-2 and Uc39-6 cells were also lower than that in Uc321 cells (data not shown). Taken together, these findings demonstrate marked reduction of vimentin expression in HCV core-expressing cell lines.

Cellular vimentin content affects the protein level of HCV core protein

To investigate the relationship between HCV core protein and vimentin, we examined the effect of cellular vimentin content on level of HCV core protein. When the expression of vimentin or control hypoxanthine guanine phosphoribosyltransferase 1 (HPRT) was knocked down in Uc39-6 cells by siRNA treatment, the protein level of HCV core protein in vimentin-knocked-down cells was significantly higher than those in siRNA-untreated and HPRT-knocked-down cells (Fig. 3A). On the other hand, cellular mRNA levels of HCV core protein, corrected for β-actin mRNA content, did not differ substantially among these types of cells (Table 1). These findings revealed that post-translational steps were involved in the increase of HCV core protein level in vimentin-knocked-down cells. Next, we established a vimentin-overexpressing Huh7 cell line, Huh7/vimentin, and compared the level of the core protein in Huh7/vimentin cells with that in control Huh7/hygro cells after transient expression of the core protein with pcEF39neo vector. After 9-day culture with G418 selection, the viabilities of the two types of cells were similar, though the level of expression of the core protein in Huh7/vimentin was significantly lower than that in Huh7/hygro cells (Fig. 3B). These findings demonstrated that level of HCV core protein was inversely correlated with cellular vimentin content, and thus strongly suggested that it was affected by cellular vimentin content.

We further attempted to verify these effects of vimentin using the vimentin-null cell line 1HF5 and the vimentin-expressing control cell line 2CB5, derived from human adrenal carcinoma SW13 cells (Sarria et al., 1990). When 1HF5 and 2CB5 cells were transfected with the core expression vector pcEF39neo and cultured with G418 selection, the viabilities of the two types of cells were similar, though the level of expression of the core protein in 1HF5 cells was much higher than that in 2CB5 cells (Fig. 3C), consistent with the results in Figs. 3A, B. An exogenously vimentin-expressing 1HF5 cell line carrying pcDNA3.1/Hygro/vimentin, 1HF5/vimentin, and a control vimentin-null cell line carrying pcDNA3.1/Hygro, 1HF5/hygro, were then established, and transfected with the green fluorescent protein (GFP)-expressing pcDNA3.1/EGFP vector, the core-coding pcEF39neo vector, or the control pcFE321swxneo vector. After selection under G418 for 9 days, the viabilities of these transfected cells were nearly the same. The levels of expression of GFP were similar in 1HF5/hygro and 1HF5/vimentin cells, while the core protein level in 1HF5/vimentin cells was significantly lower than that in 1HF5/hygro cells (Fig. 3D), consistent with the results in Fig. 3B.

These findings together indicate that cellular vimentin content regulates the level of HCV core protein in post-translational fashion.

Vimentin is involved in proteasomal degradation of core proteins in cells

HCV core proteins are known to be preferentially degraded by the proteasome-dependent pathway (Suzuki et al., 2001). To determine whether cellular vimentin content affects proteasome-dependent degradation of the core protein, we examined the effects of the proteasome inhibitor MG132 on core protein levels in vimentin-knocked-down cells. After Huh7 cells transfected with pCAG/Flag-core (Huh7/Flag-core cells) had been treated with MG132 for 16 h, cellular accumulation of core protein was analyzed by immunoblot (Fig. 4; lanes 3 vs 4), which indicated substantial proteasomal degradation of the core proteins in cultured cells, as described previously (Hope and McLauchlan, 2000; McLauchlan et al., 2002; Suzuki et al., 2001). Huh7/Flag-core cells transfected with control and HPRT siRNA duplexes exhibited similar increases in core protein levels by treatment with MG132 (Fig. 4; lanes 5 vs 6, and 9 vs 10). On the other hand, vimentin-knocked-down Huh7/Flag-core cells that were transfected with vimentin siRNA duplexes exhibited higher content of core protein (lane 7) than the other siRNA-treated cells (lanes 5 and 9), and MG132 treatment resulted in no significant difference in core protein levels in vimentin-knocked-down cells (lanes 7 and 8), indicating that proteasomal degradation of core proteins was markedly inhibited in the vimentin-knocked-down cells. These observations strongly suggested that vimentin plays an important role in the proteasome-mediated proteolytic pathway of the HCV core protein.

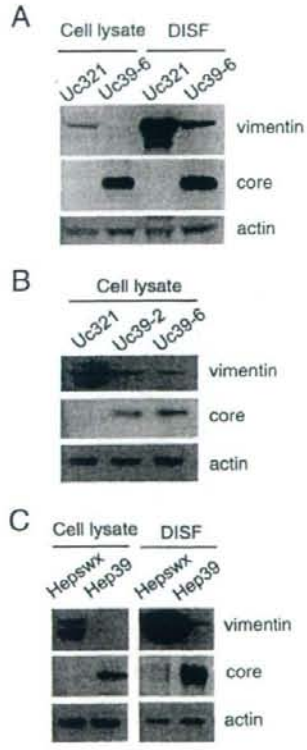

Fig. 2. Immunoblot analysis of vimentin in HCV core-expressing cell lines. Cell lysate fractions and DISFs from various cell lines were analyzed by immunoblotting with antibodies to vimentin, HCV core protein, and β-actin as indicated: cell lysate fractions and DISFs from Uc321 and Uc39-6 cells in (A), cell lysate fractions from Uc321, Uc39-2, and Uc39-6 cells in (B), and cell lysate fractions and DISFs from Hepswx and Hep39 cells in (C). Amounts of protein loaded were 18 μg in (A) and (B), and 5 μg in (C).

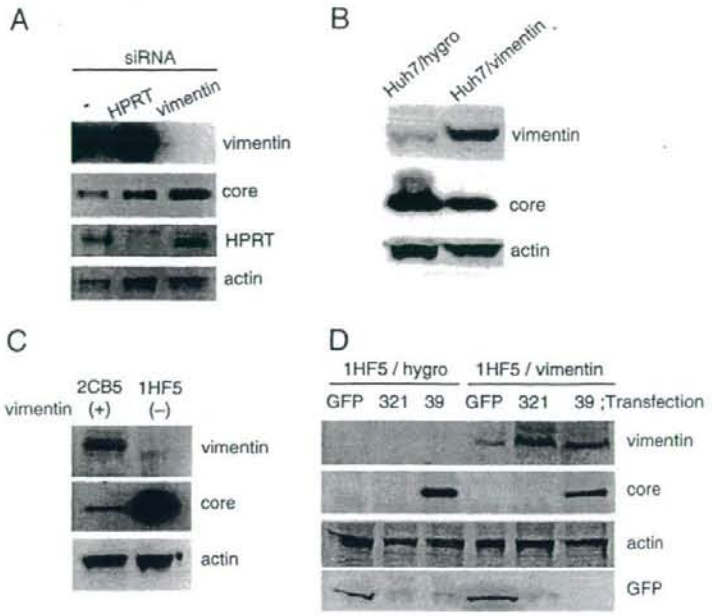

Fig. 3. Effects of cellular vimentin content on the level of expression of HCV core protein. Cellular level of expression of vimentin, HCV core protein, HPRT, β-actin, and GFP were analyzed by immunoblotting of total cell lysates (40 μg of protein) from various cells using specific antibodies. (A) Uc39-6 cells were transfected twice with a 2-day interval without (–) or with vimentin or control HPRT siRNA duplexes. Four days after the first transfection, cell lysates were collected and analyzed. (B) Huh7/hygro and Huh7/vimentin cells were transfected with the core protein-expression vector pcEF39neo, and selected under 1 mg/ml of G418 for 9 days. (C) The 2CB5 (vimentin+) and 1HF5 (vimentin−) lines of SW13 cells were transfected with pcEF39neo, and selected under 1 mg/ml of G418 for a week, followed by additional 2-week culture in normal culture medium. (D) 1HF5/hygro and 1HF5/vimentin cells were transfected with pcDNA3.1/EGFP (GFP), pcFE321swxneo (321), or pcEF39neo (39), and selected under 1 mg/ml of G418 for 9 days.

Under the various siRNA-treated conditions in Fig. 4, we also examined the protein levels of p53, one of the endogeneous host proteins the degradation of which is mainly regulated by proteasomal system (Morimoto et al., 2008). The pattern of p53 protein levels was very similar to that of core protein levels (Fig. 4), suggesting that the vimentin-dependent proteasomal degradation is not specific for the viral core protein. Vimentin-dependent proteasomal degradation system might be generally important for the turnover of endogeneous cellular proteins as well as the viral core protein.

Cellular vimentin contents affect HCV production

Since the level of expression of HCV core protein was affected by cellular vimentin content, we examined whether HCV production was also affected by cellular vimentin content. Infectious HCV (JFH1 strain) particles were used for the following infection assays. HCV production activity was determined by quantification of HCV core protein levels in the infected cells and culture supernatants. We first tested the effect of vimentin knockdown on HCV production. Examination of HCV-infected Huh7 cells treated with vimentin siRNA revealed higher amounts of HCV core protein in both cells and culture medium than examination of non-treated and control HPRT siRNA-treated cells (Fig. 5A). To examine whether the core protein levels in the cell-cultured media reflect the content of infectious HCV particles in them, Huh7 cells were treated with cell-cultured medium containing equal amounts (1.4 fmol) of the core protein collected from each type of cell described in Fig. 5A, and cellular levels of production of the core protein were determined by immunoblot analysis. They were nearly the same among the cells treated with each culture medium (Fig. 5B). These findings indicated that reduction of vimentin expression in Huh7 cells leads to more active HCV production and enhanced release to the supernatant.

We next examined the effects of vimentin overexpression on HCV production. When vimentin-overexpressing Huh7/vimentin and control Huh7/hygro cells were infected with HCV particles, Huh7/vimentin cells exhibited lower amounts of intracellular and extracellular HCV core protein than Huh7/hygro cells (Fig. 5C). Consistent with the results in Fig. 5A, these findings suggested that higher expression of vimentin in host cells resulted in lower HCV production.

We also examined the effect of vimentin knockdown on HCV RNA replication using a JFH1-subgenomic replicon (Fig. 5D). There were no significant differences in replication activities between vimentin-knocked-down cells and the other control cells. These findings indicated that cellular level of vimentin has no effects on HCV non-structural proteins which serve as a unit of RNA replication machinery of HCV. Collectively, these results demonstrated that HCV production activity but not HCV-RNA replication was inversely correlated with cellular vimentin content.

Table 1
mRNA levels of HCV core protein and β-actin in vimentin-knocked-down Uc39-6 cells

	siRNA		
	–	HPRT	vimentin
HCV core ($\times 10^4$ copies/μg total RNA)	2.9±0.3	1.7±0.1	3.0±0.2
β-actin ($\times 10^7$ copies/μg total RNA)	3.0±0.1	1.4±0.1	2.3±0.0
HCV core/β-actin[a]	1	1.3	1.3

Total RNA was isolated from Uc39-6 cells that had been treated twice with a 2-day interval with HPRT siRNA duplexes, with vimentin siRNA duplexes or without (–) either of them, and cultured for 4 days. mRNA levels of HCV core protein and β-actin (a control housekeeping gene) were determined by quantitative real-time PCR. Values are the mean ± SD for three determinations.

[a] Numbers represent the relative amounts of HCV core protein mRNA normalized to β-actin level.

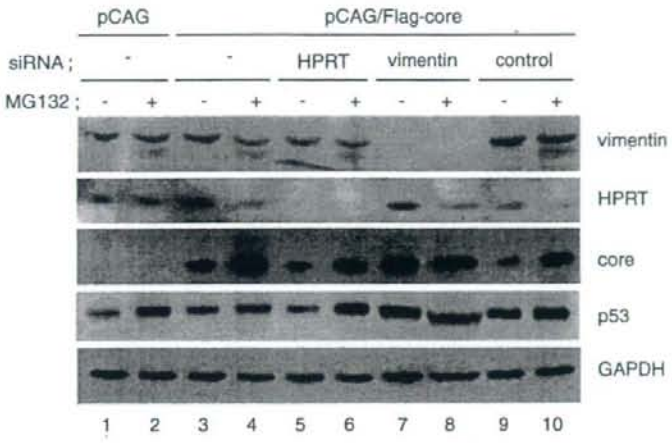

Fig. 4. Effects of the proteasome inhibitor MG132 on level of expression of HCV core protein in Huh7 cells. siRNA duplexes of control, HPRT, or vimentin, together with the core protein-expression vector pCAG/Flag-core, were transfected into Huh7 cells. After 2 days, transfection of these siRNAs was repeated. Cells were further cultured for 2 days and treated with (+) or without (−) MG132 (50 μM) for 16 h. Equivalent amounts of cell lysates were analyzed by immunoblotting with antibodies to vimentin, HPRT, core protein, p53, and GAPDH.

Furthermore, expression of vimentin and HCV core protein in Huh7 cells after HCV infection was observed by immunofluorescence microscopy (Fig. 5E), and the fluorescent intensity of vimentin in core-positive and core-negative Huh7 cells under HCV-infected conditions was determined (Fig. 5F). HCV-infected cells stained with the core-specific antibody always had lower vimentin content (Figs. 5E, F). Moreover, as shown in Fig. 5F, HCV core-negative cells exhibited more variable vimentin levels, whereas the core-positive cells had vimentin levels within a narrow range. These observations, which showed that a Huh7 cell population with lower vimentin content can preferentially produce HCV, were consistent with the results shown in Figs. 5A, C.

Finally, we examined the effects of MG132 on HCV core protein levels in HCV-infected cells in which vimentin was knocked-down or overexpressed. In the presence of MG132, non-treated and control HPRT siRNA-treated cells showed the significant increase of cellular HCV core protein levels, whereas vimentin-knocked-down cells did not (Fig. 5G). These results were consistent with those using HCV core-expressing cells (Fig. 4). HCV core content in vimentin-overexpressing Huh7/vimentin cells was lower than that in control Huh7/hygro cells, but after MG132 treatment Huh7/vimentin and Huh7/hygro cells showed the similar HCV core protein levels (Fig. 5H). Taken together, these results demonstrated the significant involvement of vimentin in proteasome-dependent degradation of HCV core protein in HCV-infected cells (Figs. 5G, H), as well as in HCV core-expressing cells (Fig. 4).

Discussion

By comparative proteomic analysis of the detergent-insoluble proteins in HCV core-expressing and non-expressing Huh7 cell lines, vimentin, an intermediate filament protein, was identified as the protein with the most dramatic reduction in level in the detergent-insoluble fraction of HCV core-expressing Uc39-6 cells (Figs. 1B and 2). On the other hand, there were no significant differences in the amounts of other major proteins including cytoskeletal components such as actin and cytokeratin 8/18 in the detergent-insoluble fractions between the core-expressing and non-expressing cells (Fig. 1B). These findings, together with similar results for other core-expressing cells (Fig. 2), suggested the existence of a specific relationship between the core protein and cellular vimentin. Consistent with these findings, immunofluorescence microscopic analysis of core-expressing cells (data not shown) and HCV-infected cells (Figs. 5E, F) showed that cells with intrinsic lower amount of vimentin are more permissive for higher HCV core protein content.

Knockdown of vimentin expression by siRNA treatment resulted in an increase in HCV core protein levels (Fig. 3A), while overexpression of vimentin reduced core protein contents (Fig. 3B). Similar results were obtained in the experiments using the vimentin-null cell line 1HF5 derived from SW13 cells (Figs. 3C and D). On the other hand, transient knockdown and overexpression of the core proteins in Uc39-6 and Huh7 cells, respectively, did not result in differences in cellular vimentin content (data not shown). These findings indicated that cellular vimentin level affects the level of expression of the core protein but not vice versa. Although transient expression of the core protein did not affect cellular vimentin content, why do various stable cell lines expressing the core protein have lower vimentin level? Since it was very hard to establish the cells stably expressing the core protein, we speculate that only the minor cell population innately having lower vimentin content was able to maintain the substantial core expression levels and was therefore selected.

We next demonstrated that vimentin affects core protein levels in post-translational fashion (Table 1) and is required for the proteasomal degradation of core protein in core-expressing cells (Fig. 4) and also in HCV-infected cells (Figs. 5G, H). Many studies with proteasome inhibitors have shown that a major pathway of degradation of core protein is mediated by the proteasomal system (Hope and McLauchlan, 2000; McLauchlan et al., 2002; Moriishi et al., 2003; Suzuki et al., 2001). PA28γ, a REG family proteasome activator also known as REGγ and Ki antigen, which is located in the nucleus, was shown to play an important role in the proteasomal degradation of the core protein (Moriishi et al., 2003). It was recently reported that the ubiquitin ligase E6AP, which is distributed in the perinuclear cytoplasm and colocalized with the core protein, is also involved in ubiquitylation and degradation of core protein (Shirakura et al., 2007). Vimentin filaments extend from the nuclear membrane toward the cell periphery. In addition, vimentin is known to colocalize with ubiquitinated protein aggregates and form aggresomes when the capacity of the proteasome is exceeded (Johnston et al., 1998). Pull-down assays against the core protein in core-expressing Huh7 cells indicated that a minor portion of cellular vimentin can interact with HCV core protein (data not shown), as

Kang et al. had reported previously (Kang et al., 2005). Co-staining of cellular vimentin and the core protein on immunofluorescence microscopy also supported the existence of a minor but definite association between them (data not shown). Based on these findings, we speculate that vimentin plays a role in the transport of the core protein to the nucleus, where it is then degraded, although further biochemical studies will be needed to demonstrate this.

HCV core protein is distributed mainly in the ER and lipid droplets in host cells (Barba et al., 1997), and the ER membrane associating the lipid droplets with core protein has been recognized as a site important for HCV production, particularly HCV RNA replication and virus particle assembly (Boulant et al., 2007; Miyanari et al., 2007). Vimentin is also closely associated with lipid droplets (Brasaemle et al., 2004; Lieber and Evans, 1996; Schweitzer and Evans, 1998). Thus, in addition to its degradative modulation of core protein, vimentin might also affect the function of lipid droplets and consequently inhibit HCV production. The effects of vimentin knock-down and overexpression on HCV production were actually stronger at the extracellular core protein level (secretion

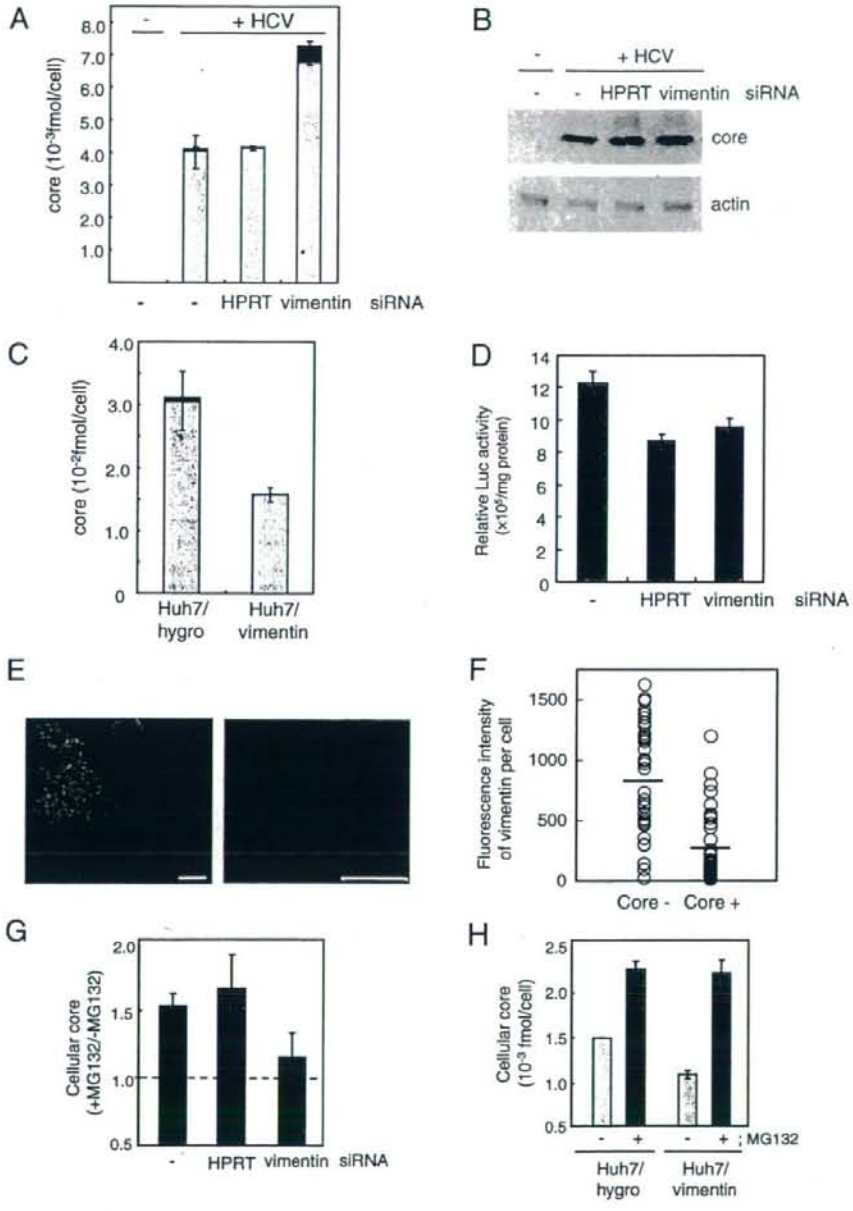

of the virus) than at the intracellular core protein level (Figs. 5A, C), suggesting additional activity of vimentin in the processes of HCV particle release.

Since the level of expression of vimentin in carcinomas is correlated with parameters of malignant potential such as tumor grade and tumor invasion, vimentin has been used as a marker of malignant tumors (Bannasch et al., 1982). It has indeed been reported that some HCV-infected patients with hepatocellular carcinoma exhibited up-regulation of vimentin expression in tumor tissue (Kim et al., 2003) although further statistical studies are required to clearly demonstrate this. Tanaka et al. noted that in livers of HCV-infected patients with hepatocelllular carcinoma the virus existed predominantly in non-cancerous tissue, at levels 10- to 100-fold higher than in cancerous tissue (Tanaka et al., 2004). These observations in human liver samples suggest that the reduction in HCV levels in hepatic tumor can be explained by the increase of vimentin expression in tumor, consistent with our findings for cultured cells.

In this study we demonstrated that cellular vimentin expression enhanced the proteasomal degradation of core protein and eventually restricted HCV production. Vimentin itself and sites of vimentin/core interaction may thus be novel targets of treatment using anti-HCV strategies.

Materials and methods

Antibodies

Mouse monoclonal antibodies to annexin II, fatty acid synthase, calnexin, lamin A/C, and GFP were purchased from BD Transduction Laboratories. Mouse monoclonal antibodies to HCV core protein, prohibitin, and glyceraldehyde-3-phosphate dehydrogenase (GAPDH) were from Anogen, Lab Vision, and Abcam, respectively. Rabbit polyclonal antibodies to vimentin, lamin B1, p53, and HPRT were from Santa Cruz Biotechnology Inc., while those to actin were from Biomedical Technologies Inc.

Plasmids

The mammalian expression vector of HCV core protein, pcEF39neo (Ruggieri et al., 1997), and the empty vector pcEF321swxneo (Harada et al., 1995) were described previously. The mammalian expression vector of Flag-tagged HCV core protein, pCAG/Flag-core, and the empty vector, pCAG, were described previously (Moriishi et al., 2003). For construction of a mammalian expression vector of vimentin, pcDNA3.1/Hygro/vimentin, vimentin fragment was amplified by PCR using the reverse-transcribed cDNAs of Huh7 cells as a template. The PCR primer pairs used were 5′-GCCATGTCCACCAGGTCCGTGTCC-3′ and 5′-TTATTATTCAAGGTCATCGTGATG-3′. The PCR products were inserted into the EcoRV site of pBluescript SKII(+). pBluescript SK(+)/vimentin was digested with Hind III and Xba I, and the vimentin fragment was inserted into pcDNA3.1/Hygro (Invitrogen), which had been digested with Hind III and Xba I. For construction of pcDNA3.1/EGFP, EGFP fragment was prepared by digestion of pEGFP-N1 (Clontech Laboratories, Inc.) with Nhe I and Hind III and inserted into pcDNA3.1/Hygro, which had been digested with Nhe I and Hind III. The subgenomic replicon constructs, pSGR-JFH1/Luc (wild type) and pSGR-JFH1/Luc-GND (GND mutation in the NS5B sequence), with the firefly luciferase reporter gene were described previously (Kato et al., 2005).

Cell lines

All hepatic cells used in this study were plated on collagen-coated dishes (Asahi Techno Glass, Japan). Human hepatic Huh7 and Huh7.5.1 cells were grown in normal culture medium [Dulbecco's modified Eagle's medium (DMEM) (KOJIN BIO, Japan) supplemented with 10% fetal bovine serum (FBS), 100 U/ml Penicillin G, and 100 mg/ml streptomycin sulfate] containing 0.1 mM non-essential amino acids (GIBCO) under a 5% CO_2 atmosphere at 37 °C. We used human hepatic cell lines constitutively expressing HCV core protein, including Hep39 from HepG2 cells (Harada et al., 1995; Ruggieri et al., 1997) and Uc39-2 and Uc39-6 from Huh7 cells (Fukasawa et al., 2006; Sato et al., 2006). Huh7 and HepG2 cell lines carrying the empty vector, Hepswx and Uc321, respectively, were used as a mock control. All of these stable transfectants were maintained in normal culture medium containing 1 mg/ml G418 (Sigma). The human adrenal carcinoma cell line SW13, the subtypes 2CB5 and 1HF5 of which do or do not express vimentin, respectively (Sarria et al., 1990), was maintained in normal culture medium. When the pcDNA3.1/EGFP vector was transfected into 2CB5 and 1HF5 cells, the percentage of GFP-positive cells was 56.3% and 53.6%, respectively, 2 days after transfection ($n=3$), indicating that there was no difference in the transfection efficiency between these cells. To establish vimentin-overexpressing cells, pcDNA3.1/Hygro/vimentin was transfected into 1HF5 and Huh7 cells using FuGENE 6 transfection regent (Roche). The vimentin-overexpressing Huh7 and 1HF5 cells were selected under hygromycin for 2 weeks and cloned to obtain Huh7/vimentin cells and 1HF5/vimentin cells, respectively. Huh7 and 1HF5 cells carrying the empty vector pcDNA/Hygro were also established, as Huh7/hygro cells and 1HF5/hygro cells, respectively.

Preparation of DISFs

Confluent monolayers of Uc321 and Uc39 cells in four culture dishes (150 mm inner diameter) were harvested by trypsinization, and 1.5×10^7 cells of each were pelleted by centrifugation (218 ×g for 5 min at 4 °C). After washing with PBS three times, each cell pellet was resuspended in 1 ml of lysis buffer [10 mM HEPES-HCl, pH 7.5, 10 mM NaCl, 140 mM KCl, 0.5 mM DTT, 0.5% Triton X-100 (Pierce Biotechnology), 10 mM NaF, Complete™ EDTA-free (Roche)] (i.e. a 20% cell suspension). The cell suspension was lysed with a ball-bearing homogenizer (Hope et al., 2002). The soluble fraction (designated the detergent-soluble fraction, DSF) containing ~85% of the total cellular proteins was collected by centrifugation of the cell

Fig. 5. HCV production in vimentin-knockdown and vimentin-overexpressing Huh7 cells. (A) Huh7 cells (5×10^4 cells) in 48-well plates were incubated with or without HCV particles (including 8.0 fmol of core protein) for 6 h, and then treated twice with a 3-day interval without (−) or with siRNA duplexes of HPRT or vimentin. After 7-day culture, the amounts of HCV core protein per cell in cells (light gray bar) and culture medium (dark gray bar) were determined. $n=3$. (B) Culture medium was collected at day 6 in the infection experiment described above in (A). The concentration of HCV core protein in these samples of medium was adjusted to 2.7 fmol/ml with fresh medium. Cells were infected with these samples of medium containing 1.4 fmol of HCV core protein for 2 days, and harvested after 7-day incubation. Infectivity was analyzed by the immunoblotting of cell lysates with antibodies to HCV core protein and β-actin. (C) Vimentin-overexpressing Huh7/vimentin and control Huh7/hygro cells infected with HCV were harvested after 7-day incubation. The amounts of HCV core protein per cell in cells (light gray bar) and culture medium (dark gray bar) were determined. (D) Huh7 cells harboring the HCV subgenomic replicon containing a luciferase reporter gene were transfected without (−) or with siRNA duplexes of HPRT or vimentin. After 2.5-day culture, luciferase activity in cell extracts was determined. $n=3$. (E) Immunofluorescence microscopic analysis of HCV-infected Huh7 cells. After infection with HCV, Huh7 cells were cultured for 6 days. HCV core protein (green) and vimentin (red) were then detected with specific antibodies. Nuclei (blue) were stained with DAPI. Two views showing low and high magnifications are displayed. Bars, 100 μm in the left panel; 50 μm in the right panel. (F) Under the HCV-infected conditions in panel E, fluorescence intensity of vimentin in core-positive and core-negative Huh7 cells was determined by line profile analysis. $n=40$. Statistical significance of differences in fluorescence intensity of vimentin between core-positive and core-negative cells was evaluated using Student's t test, showing $p<10^{-8}$. (G) As in (A), Huh7 cells were incubated with HCV particles, and then treated twice with a 2-day interval without (−) or with siRNA duplexes of HPRT or vimentin. After 4.5-day culture, cells were treated with (+) or without (−) MG132 (50 μM) for 16 h. In each culture condition, the ratio of HCV core protein level in the MG132-treated cells to that in MG132-untreated cells was determined. $n=3$. (H) Huh7/vimentin and Huh7/hygro cells infected with HCV were cultured for 4 days and treated with (+) or without (−) MG132 (50 μM) for 16 h. The amounts of cellular core protein per cell were determined. $n=3$.

lysate performed twice at 218 ×g for 5 min at 4 °C. The insoluble pellet was suspended in 2 ml of lysis buffer containing 1.62 M sucrose and then centrifuged at 10,000 ×g for 1 h at 4 °C. The pellet was resuspended in 1 ml of lysis buffer containing 1.0 M sucrose and layered over 2 ml of lysis buffer containing 2.0 M sucrose. After centrifugation at 50,000 ×g for 2 h at 4 °C, the precipitated fraction containing ~15% of total cellular proteins was collected and resuspended in lysis buffer containing 0.25 M sucrose at a concentration of 3 mg protein/ml (designated the detergent-insoluble fraction, DISF). Each fraction was stored at −80 °C until use. The protein concentrations in these preparations were determined with BCA protein assay reagents (Pierce Biotechnology) using BSA as a standard.

2D-PAGE/MALDI-QIT-TOF MS analysis

The DISF (0.15 mg protein) of each cell line was cleaned using a PlusOne™ 2-D Clean Up kit (GE Healthcare) and resuspended in rehydration solution containing 9 M urea, 4% CHAPS, 65 mM dithioerythritol, and 0.5% ampholyte. The first-dimensional IEF was performed with an Immobiline Dry Strip pH 4–7 according to the manufacturer's instruction (GE Healthcare). The second-dimensional electrophoresis was carried out on 12% SDS-polyacrylamide gel, and the gel was stained with SYPRO-Ruby (Bio-Rad). Spot detection and comparison in 2D images were accomplished with PDQuest™ 2-D analysis software ver. 7.3 (Bio-Rad). The protein bands were excised from the gel and subjected to in-gel trypsin digestion. The tryptic peptide mixtures were analyzed by MALDI-QIT-TOF MS (AXIMA-QIT, Shimazu Biotech, Japan) as described previously (Sato et al., 2006; Shevchenko et al., 1996). Mascot software (Matrix Science) was used for protein identification.

Immunoblot analysis

The proteins were separated by electrophoresis in precast NuPAGE 10% or 12% Bis–Tris gels (Invitrogen), and then transferred to a polyvinylidene difluoride membrane. The membranes were blocked overnight at 4 °C or for 60 min at room temperature in Tris-buffered saline containing 0.1% Tween 20 and 5% skim milk. The blots were probed with the first antibodies at 1:1000 dilution for 60 min at room temperature and then incubated with horseradish peroxidase (HRP)-conjugated goat anti-rabbit IgG (Bio-Rad) or HRP-conjugated goat anti-mouse IgG (GE Healthcare) at 1:2000 dilution for 45 min. Detection of immunoreactive proteins was performed using an ECL system (GE Healthcare).

Quantitative real-time PCR analysis

Cellular total RNAs were prepared with an RNeasy kit (Qiagen). The total RNA fraction (1 μg) was processed directly to cDNA using a Transcriptor First Strand cDNA Synthesis Kit (Roche). Of the total 20 μl cDNA solution, an aliquot of 0.5–2 μl was used for each real-time PCR assay. The PCR primers used for HCV core protein were: forward, 5′-AGGAAGACTTCCGAGCG-3′, and reverse, 5′-GGGTGACAGGAGCCATC-3′. The PCR primers for actin were obtained from the LightCycler™-Primer Set (Roche). Quantitative real-time PCR was carried out in a LightCycler (Roche) using LightCycler-FastStart DNA Master SYBR Green I (Roche).

Transfection of siRNA

Subconfluent cells cultured in a 48-well plate were transfected twice at a 2- or 3-day interval with 30 nM of vimentin-specific, HPRT-specific, or negative control (Invitrogen) siRNA duplexes using Lipofectamine RNAiMAX (Invitrogen) following the manufacturer's instructions. The siRNA target sequences were as follows: vimentin (sense), 5′-ACCTTGAACGCAAAGTGGAATCTTT-3′; HPRT-S1 (sense), 5′-AAGCCAGACUUUGUUGGAUUUGAAA-3′.

Infection of Huh7 cells with HCV

Infectious HCV (JFH1 strain) particles were produced in Huh7.5.1 cells as described previously (Wakita et al., 2005). Culture supernatant containing infectious HCV particles was collected and stored at −80 °C until use. Subconfluent naïve Huh7, Huh7/hygro, or Huh7/vimentin cells in 24-well or 48-well plates were exposed to normal culture medium containing HCV particles (1.4–8 fmol core protein/well, corresponding to moi = 0.0175–0.1) for 6 h at 37 °C. Cells were then washed and maintained in 500 μl (24-well) or 250 μl (48-well) of normal culture medium for 6–7 days at 37 °C. To determine HCV production activity, the amounts of HCV core protein in the culture medium and cell lysates were quantified with an enzyme-linked immunosorbent assay (ELISA) (Ortho® HCV antigen ELISA test, Ortho-Clinical Diagnostics, Japan).

Assay for activity of HCV genomic RNA replication

The RNAs (30 μg) transcribed from pSGR-JFH1/Luc and pSGR-JFH1/Luc-GND (Kato et al., 2005) were transfected into Huh7 cells (1.6×10^6 cells) by electroporation. Transfected cells in normal culture medium were immediately seeded into 48-well plates at 9.0×10^4 cells/well. Four hours after transfection, siRNAs were also transfected into these cells. After incubation for 2.5 days, cells were harvested and the luciferase activity in cell lysates was determined with the Luciferase Assay System (Promega). Since the luciferase activities of the JFH1/Luc replicon were ~400-fold higher than those of the JFH1/Luc-GND mutant replicon, background luciferase activity, which is independent of replication activity, was very low in our experimental conditions.

Immunofluorescence microscopy

Cells cultured on glass cover slips (in 24-well plates) were fixed in 1% formaldehyde-PBS for 1 h at 4 °C, permeabilized in PBS containing 0.1% Triton X-100 for 5 min, and washed twice with PBS. The cell monolayers were incubated with rabbit anti-vimentin antibodies (1:100) and mouse anti-HCV core protein antibodies (1:100) for 60 min at room temperature. After washing with PBS, the cells were incubated with Alexa488-conjugated anti-mouse IgG, Alexa594-conjugated anti-rabbit IgG, and DAPI (4′, 6′-diamidino-2-phenylindole) (Invitrogen) for 60 min at 4 °C. Coverslips were washed with PBS and mounted on glass slides. Immunofluorescence was visualized and quantitated with a confocal laser-scanning microscope (Axiovert 100M, Carl Zeiss) equipped with a LSM510 system (Carl Zeiss).

Acknowledgments

Huh-7.5.1 cells and Huh-7 cells were kindly provided by F. V. Chisari (Scripps Research Institute).

This work was supported in part by grants-in-aid from the Ministry of Health, Labor, and Welfare of Japan, and by grants-in-aid from the Ministry of Education, Culture, Sports, Science, and Technology of Japan.

References

Aizaki, H., Lee, K.J., Sung, V.M., Ishiko, H., Lai, M.M., 2004. Characterization of the hepatitis C virus RNA replication complex associated with lipid rafts. Virology 324 (2), 450–461.

Ariumi, Y., Kuroki, M., Abe, K., Dansako, H., Ikeda, M., Wakita, T., Kato, N., 2007. DDX3 DEAD-box RNA helicase is required for hepatitis C virus RNA replication. J. Virol. 81 (24), 13922–13926.

Bannasch, P., Zerban, H., Mayer, D., 1982. The cytoskeleton in tumor cells. Pathol. Res. Pract. 175 (2–3), 196–211.

Barba, G., Harper, F., Harada, T., Kohara, M., Goulinet, S., Matsuura, Y., Eder, G., Schaff, Z., Chapman, M.J., Miyamura, T., Brechot, C., 1997. Hepatitis C virus core protein shows a cytoplasmic localization and associates to cellular lipid storage droplets. Proc. Natl. Acad. Sci. U. S. A. 94 (4), 1200–1205.

Bartenschlager, R., Lohmann, V., 2000. Replication of hepatitis C virus. J. Gen. Virol. 81 (Pt 7), 1631–1648.
Boulant, S., Targett-Adams, P., McLauchlan, J., 2007. Disrupting the association of hepatitis C virus core protein with lipid droplets correlates with a loss in production of infectious virus. J. Gen. Virol. 88 (Pt 8), 2204–2213.
Brasaemle, D.L., Dolios, G., Shapiro, L., Wang, R., 2004. Proteomic analysis of proteins associated with lipid droplets of basal and lipolytically stimulated 3T3-L1 adipocytes. J. Biol. Chem. 279 (45), 46835–46842.
Choo, Q.L., Kuo, G., Weiner, A.J., Overby, L.R., Bradley, D.W., Houghton, M., 1989. Isolation of a cDNA clone derived from a blood-borne non-A, non-B viral hepatitis genome. Science 244 (4902), 359–362.
Fukasawa, M., Tanaka, Y., Sato, S., Ono, Y., Nitahara-Kasahara, Y., Suzuki, T., Miyamura, T., Hanada, K., Nishijima, M., 2006. Enhancement of de novo fatty acid biosynthesis in hepatic cell line Huh7 expressing hepatitis C virus core protein. Biol. Pharm. Bull. 29 (9), 1958–1961.
Harada, T., Kim, D.W., Sagawa, K., Suzuki, T., Takahashi, K., Saito, I., Matsuura, Y., Miyamura, T., 1995. Characterization of an established human hepatoma cell line constitutively expressing non-structural proteins of hepatitis C virus by transfection of viral cDNA. J. Gen. Virol. 76 (Pt 5), 1215–1221.
Hope, R.G., McLauchlan, J., 2000. Sequence motifs required for lipid droplet association and protein stability are unique to the hepatitis C virus core protein. J. Gen. Virol. 81 (Pt 8), 1913–1925.
Hope, R.G., Murphy, D.J., McLauchlan, J., 2002. The domains required to direct core proteins of hepatitis C virus and GB virus-B to lipid droplets share common features with plant oleosin proteins. J. Biol. Chem. 277 (6), 4261–4270.
Johnston, J.A., Ward, C.L., Kopito, R.R., 1998. Aggresomes: a cellular response to misfolded proteins. J. Cell Biol. 143 (7), 1883–1898.
Kang, S.M., Shin, M.J., Kim, J.H., Oh, J.W., 2005. Proteomic profiling of cellular proteins interacting with the hepatitis C virus core protein. Proteomics 5 (8), 2227–2237.
Kato, T., Date, T., Miyamoto, M., Sugiyama, M., Tanaka, Y., Orito, E., Ohno, T., Sugihara, K., Hasegawa, I., Fujiwara, K., Ito, K., Ozasa, A., Mizokami, M., Wakita, T., 2005. Detection of anti-hepatitis C virus effects of interferon and ribavirin by a sensitive replicon system. J. Clin. Microbiol. 43 (11), 5679–5684.
Kim, W., Oe Lim, S., Kim, J.S., Ryu, Y.H., Byeon, J.Y., Kim, H.J., Kim, Y.I., Heo, J.S., Park, Y.M., Jung, G., 2003. Comparison of proteome between hepatitis B virus- and hepatitis C virus-associated hepatocellular carcinoma. Clin. Cancer Res. 9 (15), 5493–5500.
Kuo, G., Choo, Q.L., Alter, H.J., Gitnick, G.L., Redeker, A.G., Purcell, R.H., Miyamura, T., Dienstag, J.L., Alter, M.J., Stevens, C.E., et al., 1989. An assay for circulating antibodies to a major etiologic virus of human non-A, non-B hepatitis. Science 244 (4902), 362–364.
Lieber, J.G., Evans, R.M., 1996. Disruption of the vimentin intermediate filament system during adipose conversion of 3T3-L1 cells inhibits lipid droplet accumulation. J. Cell. Sci. 109 (Pt 13), 3047–3058.
Matto, M., Rice, C.M., Aroeti, B., Glenn, J.S., 2004. Hepatitis C virus core protein associates with detergent-resistant membranes distinct from classical plasma membrane rafts. J. Virol. 78 (21), 12047–12053.
McLauchlan, J., Lemberg, M.K., Hope, G., Martoglio, B., 2002. Intramembrane proteolysis promotes trafficking of hepatitis C virus core protein to lipid droplets. EMBO J. 21 (15), 3980–3988.
Miyanari, Y., Atsuzawa, K., Usuda, N., Watashi, K., Hishiki, T., Zayas, M., Bartenschlager, R., Wakita, T., Hijikata, M., Shimotohno, K., 2007. The lipid droplet is an important organelle for hepatitis C virus production. Nat. Cell Biol. 9 (9), 1089–1097.
Moriishi, K., Okabayashi, T., Nakai, K., Moriya, K., Koike, K., Murata, S., Chiba, T., Tanaka, K., Suzuki, R., Suzuki, T., Miyamura, T., Matsuura, Y., 2003. Proteasome activator PA28gamma-dependent nuclear retention and degradation of hepatitis C virus core protein. J. Virol. 77 (19), 10237–10249.
Morimoto, T., Fujita, M., Kawamura, T., Sunagawa, Y., Takaya, T., Wada, H., Shimatsu, A., Kita, T., Hasegawa, K., 2008. Myocardial regulation of p300 and p53 by doxorubicin involves ubiquitin pathways. Circ. J. 72 (9), 1506–1511.
Moriya, K., Yotsuyanagi, H., Shintani, Y., Fujie, H., Ishibashi, K., Matsuura, Y., Miyamura, T., Koike, K., 1997. Hepatitis C virus core protein induces hepatic steatosis in transgenic mice. J. Gen. Virol. 78 (Pt 7), 1527–1531.
Moriya, K., Fujie, H., Shintani, Y., Yotsuyanagi, H., Tsutsumi, T., Ishibashi, K., Matsuura, Y., Kimura, S., Miyamura, T., Koike, K., 1998. The core protein of hepatitis C virus induces hepatocellular carcinoma in transgenic mice. Nat. Med. 4 (9), 1065–1067.
Randall, G., Panis, M., Cooper, J.D., Tellinghuisen, T.L., Sukhodolets, K.E., Pfeffer, S., Landthaler, M., Landgraf, P., Kan, S., Lindenbach, B.D., Chien, M., Weir, D.B., Russo, J.J., Ju, J., Brownstein, M.J., Sheridan, R., Sander, C., Zavolan, M., Tuschl, T., Rice, C.M., 2007. Cellular cofactors affecting hepatitis C virus infection and replication. Proc. Natl. Acad. Sci. U. S. A. 104 (31), 12884–12889.
Reed, K.E., Rice, C.M., 2000. Overview of hepatitis C virus genome structure, polyprotein processing, and protein properties. Curr. Top. Microbiol. Immunol. 242, 55–84.
Ruggieri, A., Harada, T., Matsuura, Y., Miyamura, T., 1997. Sensitization to Fas-mediated apoptosis by hepatitis C virus core protein. Virology 229 (1), 68–76.
Sarria, A.J., Nordeen, S.K., Evans, R.M., 1990. Regulated expression of vimentin cDNA in cells in the presence and absence of a preexisting vimentin filament network. J. Cell Biol. 111 (2), 553–565.
Sato, S., Fukasawa, M., Yamakawa, Y., Natsume, T., Suzuki, T., Shoji, I., Aizaki, H., Miyamura, T., Nishijima, M., 2006. Proteomic profiling of lipid droplet proteins in hepatoma cell lines expressing hepatitis C virus core protein. J. Biochem. (Tokyo) 139 (5), 921–930.
Schweitzer, S.C., Evans, R.M., 1998. Vimentin and lipid metabolism. Sub-cell. Biochem. 31, 437–462.
Shevchenko, A., Wilm, M., Vorm, O., Jensen, O.N., Podtelejnikov, A.V., Neubauer, G., Shevchenko, A., Mortensen, P., Mann, M., 1996. A strategy for identifying gel-separated proteins in sequence databases by MS alone. Biochem. Soc. Trans. 24 (3), 893–896.
Shi, S.T., Lee, K.J., Aizaki, H., Hwang, S.B., Lai, M.M., 2003. Hepatitis C virus RNA replication occurs on a detergent-resistant membrane that cofractionates with caveolin-2. J. Virol. 77 (7), 4160–4168.
Shirakura, M., Murakami, K., Ichimura, T., Suzuki, R., Shimoji, T., Fukuda, K., Abe, K., Sato, S., Fukasawa, M., Yamakawa, Y., Nishijima, M., Moriishi, K., Matsuura, Y., Wakita, T., Suzuki, T., Howley, P.M., Miyamura, T., Shoji, I., 2007. E6AP ubiquitin ligase mediates ubiquitylation and degradation of hepatitis C virus core protein. J. Virol. 81 (3), 1174–1185.
Suzuki, R., Tamura, K., Li, J., Ishii, K., Matsuura, Y., Miyamura, T., Suzuki, T., 2001. Ubiquitin-mediated degradation of hepatitis C virus core protein is regulated by processing at its carboxyl terminus. Virology 280 (2), 301–309.
Suzuki, T., Ishii, K., Aizaki, H., Wakita, T., 2007. Hepatitis C viral life cycle. Adv. Drug Deliv. Rev. 59 (12), 1200–1212.
Tanaka, T., Inoue, K., Hayashi, Y., Abe, A., Tsukiyama-Kohara, K., Nuriya, H., Aoki, Y., Kawaguchi, R., Kubota, K., Yoshiba, M., Koike, M., Tanaka, S., Kohara, M., 2004. Virological significance of low-level hepatitis B virus infection in patients with hepatitis C virus associated liver disease. J. Med. Virol. 72 (2), 223–229.
Wakita, T., Pietschmann, T., Kato, T., Date, T., Miyamoto, M., Zhao, Z., Murthy, K., Habermann, A., Krausslich, H.G., Mizokami, M., Bartenschlager, R., Liang, T.J., 2005. Production of infectious hepatitis C virus in tissue culture from a cloned viral genome. Nat. Med. 11 (7), 791–796.

Chemistry & Biology

Messenger RNA-Programmed Incorporation of Multiple N-Methyl-Amino Acids into Linear and Cyclic Peptides

Takashi Kawakami,[1] Hiroshi Murakami,[2] and Hiroaki Suga[1,2,*]
[1]Department of Chemistry and Biotechnology, Graduate School of Engineering, The University of Tokyo, Tokyo 113-8656, Japan
[2]Research Center for Advanced Science and Technology, The University of Tokyo, Tokyo 153-0894, Japan
*Correspondence: hsuga@rcast.u-tokyo.ac.jp
DOI 10.1016/j.chembiol.2007.12.008

SUMMARY

Natural peptide products often contain N-methylated backbones, and such a modification plays a crucial role in making natural peptides peptidase resistant and membrane permeable. Here, we demonstrate the ribosomal synthesis of N-methyl-peptides by means of genetic code reprogramming. Two key technologies, a ribozyme-based de novo tRNA acylation (flexizyme) system and an *E. coli* reconstituted cell-free translation (PURE) system, were used in order to reassign arbitrarily chosen codons to N^{α}-methylated amino acids (^{Me}aa). Using this combination, we determined the general structural requirement of "accessible" ^{Me}aa and demonstrated their multiple incorporations into the nascent peptide chain according to the assignments made on mRNA, giving linear and cyclic N-methyl-peptides in high purities. This platform technology offers a convenient tool for the construction of N-methyl-peptide libraries, potentially leading to the discovery of therapeutic peptides.

INTRODUCTION

Natural peptide products isolated from various organisms often contain N-methylated backbones (Billich and Zocher, 1990; Hornbogen and Zocher, 2005). Such a modification of peptide backbone alters the properties of the peptide bond, which confers their conformational rigidity (Sagan et al., 2004). This modification contributes to improvements in the biological properties of natural peptides, such as target affinity, proteolytic stability, and/or membrane permeability. Thus, N^{α}-methylated amino acids (^{Me}aa) are invaluable components for the synthesis of peptide libraries in screening for peptides with suitable drug-like properties for potential therapeutic use. The backbone N-methylation of these peptides are generally executed by one or more of enzymes in the multienzyme clusters, called nonribosomal peptide synthetases (NRPSs) (Billich and Zocher, 1990; Hornbogen and Zocher, 2005; Sieber and Marahiel, 2005; Walsh et al., 2001). This type of peptide synthesis machinery is known to be template independent, in contrast to the mRNA template-dependent ribosomal machinery. Unfortunately, their complexity demands an enormous effort to manipulate the systems, thereby making it difficult to generate desired peptide libraries (Baltz, 2006; Fischbach and Walsh, 2006; Hahn and Stachelhaus, 2006).

On the other hand, the translation machinery expresses peptides in an mRNA template-dependent manner, which makes this system exceptionally versatile and useful for the synthesis of peptides or proteins. Unlike NRPSs, the ordinary translation system strictly incorporates 20 proteinogenic amino acids into the nascent peptide chain. However, an appropriate manipulation of the translation apparatus enables us to incorporate nonproteinogenic amino acids into peptides (Hendrickson et al., 2004; Hohsaka and Sisido, 2002; Link et al., 2003; Wang and Schultz, 2004). A classical example is that when a nonproteinogenic amino acid is charged onto an orthogonal $tRNA_{CUA}$ (the subscript base sequence indicates the anticodon), this aminoacyl-$tRNA_{CUA}$ (aa-$tRNA_{CUA}$) is able to suppress UAG amber stop codon on mRNA; thereby, the amino acid can be incorporated into the nascent peptide at the designated site (Bain et al., 1989; Noren et al., 1989). Despite encouraging results from a number of successful examples for the incorporation of nonproteinogenic amino acids with various nonnatural side chains, it has been known that some ^{Me}aa are incorporated into a peptide chain with good or modest efficiencies, and some are not at all (Bain et al., 1991; Chung et al., 1993; Ellman et al., 1992; Gilmore et al., 1999; Karginov et al., 1997; Mendel et al., 1995; Murakami et al., 2006; Short et al., 2000). To the best of our knowledge in the literature, only three ^{Me}aa, ^{Me}Gly, ^{Me}Ala, and ^{Me}Phe, have been successfully incorporated into the nascent peptide chain by means of amber suppression. Moreover, neither incorporation of multiple ^{Me}aa nor a single ^{Me}aa with amino acids bearing noncanonical side chains has been thus far reported.

More recently, a new concept of genetic code reprogramming was introduced by Forster et al. and applied to the incorporation of nonproteinogenic amino acids into peptides (Forster et al., 2003). Genetic code reprogramming involves the reassignment of codons from proteinogenic amino acids to nonproteinogenic ones via multiple sense suppressions. Thus, this methodology enables us to simultaneously incorporate multiple nonproteinogenic amino acids into peptides, which represents a major advantage over the aforementioned amber suppression method (Forster et al., 2003; Josephson et al., 2005; Murakami et al., 2006; Ohta et al., 2007; Ohuchi et al., 2007; Tan et al., 2005).

In the context of ^{Me}aa using the sense suppressions, there were three examples in the literature (Frankel et al., 2003; Merryman and Green, 2004; Tan et al., 2004). Merryman and Green have reported that aa-tRNAs prepared by cognate aminoacyl-tRNA

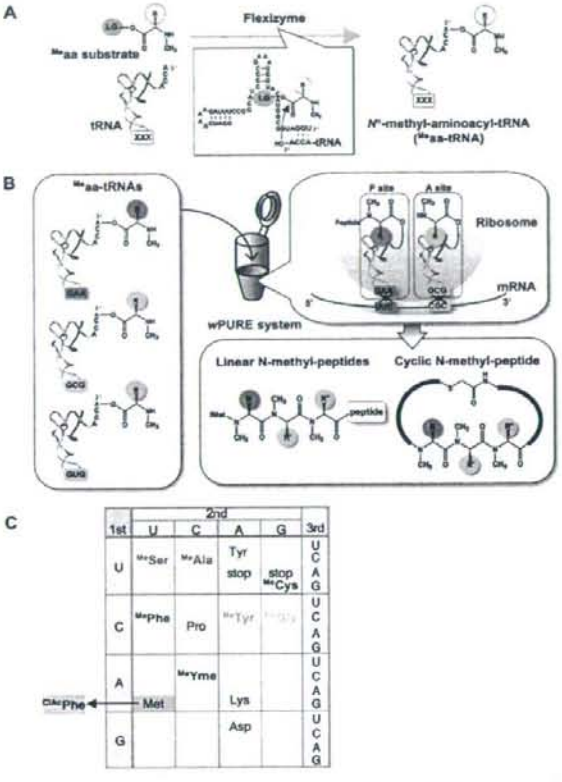

Figure 1. Messenger RNA-Programmed Synthesis of N-Methyl-Peptides by Genetic Code Reprogramming

(A) Synthesis of N^{α}-methyl-aminoacyl-tRNA (^{Me}aa-tRNA) by flexizyme system. Flexizyme recognizes leaving group (LG: highlighted in pink) on the ester bond of N^{α}-methyl-amino acid (^{Me}aa) substrate and conserved three bases on the 3′-terminus of tRNA, which allows for the aminoacylation of desired tRNA with any ^{Me}aa. N^{α}-methyl groups are highlighted in yellow.

(B) Ribosomal synthesis of N-methyl-peptide. ^{Me}aa-tRNAs bearing various combinations of ^{Me}aa and anticodon are added to the *w*PURE (*withdrawn* protein synthesis using recombinant elements) system for mRNA-programmed incorporation of ^{Me}aa into peptides. The *w*PURE system is an *E. coli* reconstituted cell-free translation system in which some components (amino acids and aminoacyl-tRNA synthases) are withdrawn from the ordinary translation system to reassign multiple sense codons to various ^{Me}aa.

(C) Reprogrammed genetic code table for the mRNA-programmed synthesis of N-methyl-peptides. Codons that are reassigned to various ^{Me}aa are shown in color letters. Initiation codon (AUG) highlighted in gray is reassigned from Met to N^{α}-(α-chloroacetyl)-Phe (^{ClAc}Phe) for the ribosomal synthesis of cyclic N-methyl-peptides.

synthetases (aaRSs) were converted to ^{Me}aa-tRNAs by the three-step procedure, where the α-amino group was alkylated by consecutive reductive amination with 2-nitrobenzaldehyde and formaldehyde, and then the 2-nitrobenzyl group was deprotected by UV irradiation (Merryman and Green, 2004). These ^{Me}aa-tRNAs derived from 20 proteinogenic amino acids were surveyed for the synthesis of a dipeptide, fMet-^{Me}aa, where thin-layer chromatographic electrophoresis was mainly used to discern the product of fMet-^{Me}aa from fMet (also possibly fMet-aa) and to determine the incorporation efficiency of each ^{Me}aa in a semiquantitative manner. In the second example, Tan and Cornish et al. prepared ^{Me}Ala-tRNA$^{AsnB}_{GAC}$ and ^{Me}Phe-tRNA$^{AsnB}_{GAC}$ by the chemoenzymatic aminoacylation procedure (Hecht et al., 1978; Robertson et al., 1991) and performed their single incorporation into a tripeptide (fMet-Xaa-Glu, where Xaa represents ^{Me}aa) upon the sense suppression of the Val codon (GUU) (Tan et al., 2004). Significantly, this work determined the incorporation efficiencies of these two ^{Me}aa into the peptide chain in a quantitative manner and also confirmed the product peptide by liquid chromatography based on its retention time by comparison with that of the corresponding synthetic authentic sample. Both examples above showed only a single incorporation of ^{Me}aa into a di- or tripeptide backbone, and therefore the concept of genetic code reprogramming has not yet been fully explored for the synthesis of N-methyl-peptides.

In the third example, Frankel and Roberts et al. have shown polymerization of ^{Me}Phe assigned to in repetition of two, five, or ten residues in an in vitro display system (Frankel et al., 2003). This work represents, to our knowledge, the first demonstration of consecutive incorporations of a single type of ^{Me}aa into a peptide stretch by using sense suppression. However, because the polymerization of ^{Me}Phe was only evidenced by observing the protease resistance of the respective peptide, it still remains unknown to what degree of the contamination of natural amino acids in the poly-^{Me}Phe chain occurred. In fact, the full-length peptide bearing multiple ^{Me}Phe was susceptible to protease to some extent, suggesting that competing incorporations of likely Val or possibly other proteinogenic amino acids occurred as Frankel et al. discussed in their report (Frankel et al., 2003). Taken together, although the above three examples clearly documented that the sense-suppression method could be used for the incorporation of ^{Me}aa, the proof-of-concept study on the genetic code reprogramming, i.e., performing multiple incorporations of two or more different ^{Me}aa with high fidelity control, remains to be demonstrated.

We report here incorporation of multiple ^{Me}aa into the peptide backbone with a nearly perfect control of sequences and lengths by using the concept of genetic code reprogramming. To reprogram the genetic code, we used two technologies, flexizyme and PURE (protein synthesis using recombinant elements) systems. Flexizyme system is a ribozyme-based de novo tRNA acylation system that is able to charge virtually any amino acids onto desired tRNAs with any body and anticodon sequences (Figure 1A) (Kourouklis et al., 2005; Murakami et al., 2003a, 2003b, 2006; Ohuchi et al., 2007; Saito et al., 2001). PURE system is a

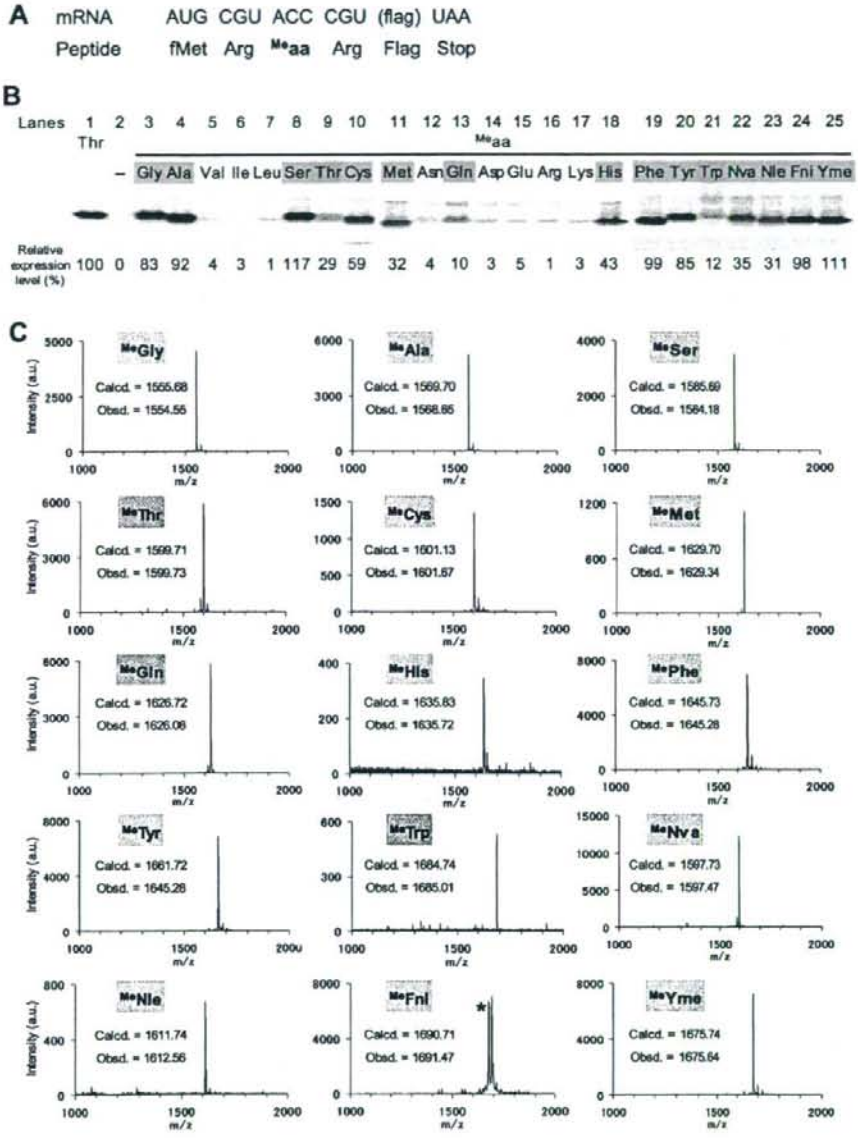

Figure 2. Single Incorporations of *N*^{Me}-Methylated Amino Acids

(A) Sequences of mRNA and peptide. Flag in parentheses indicates the RNA sequence coding the Flag peptide (DYKDDDDK).

(B) Tricine-SDS-PAGE analysis of the expressed peptides labeled with [^{14}C]-Asp detected by autoradiography. Lane 1, the wild-type peptide expressed in the ordinary PURE system where ACC assigns Thr; lane 2, a negative control using *w*PURE system in the presence of uncharged $tRNA^{Asn\text{-}E1}_{GGU}$; lanes 3–25, expression of the peptide containing a single ^{Me}aa in the presence of designated ^{Me}aa-$tRNA^{Asn\text{-}E1}_{GGU}$ prepared by the flexizyme system. Each expression level relative to wild-type was determined by a mean score of triplicates. The amino acids giving over 30% and 10% expression levels relative to the wild-type are highlighted in cyan and orange, respectively.

reconstituted *Escherichia coli* cell-free translation system in which transcription and translation are coupled (Shimizu et al., 2001). The most important feature of this translation apparatus is that some components, such as amino acids and aminoacyl-tRNA synthases (aaRSs), can be withdrawn from the translation elements (Figure 1B). By means of such a *withdrawn* PURE system, named *w*PURE, we are able to vacant certain codons at our will. Combining these two systems enables us to readily reassign the vacant codons to ^{Me}aa and express peptides as designed on mRNA sequences according to the newly designated genetic table (Figure 1C).

In this report, we initially screened *N*$^{\alpha}$-methylated proteinogenic and nonproteinogenic amino acids to evaluate the efficiency of their single incorporation into a peptide backbone. Then, we investigated the mRNA-programmed synthesis of peptides containing multiple ^{Me}aa, achieving the compositions of continuous stretches of up to ten ^{Me}aa residues. Finally, we investigated the synthesis of cyclic N-methyl-peptides closed by a physiologically stable thioether bond, showing its potential for the generation of in vivo compatible peptide libraries therapeutically targeting various proteins.

RESULTS

Single Incorporations of *N*$^{\alpha}$-Methylated Amino Acids

To investigate the incorporation of multiple ^{Me}aa into a peptide backbone, various *N*$^{\alpha}$-methylated proteinogenic and nonproteinogenic amino acids charged onto a tRNA by the flexizyme system were comprehensively evaluated for the efficiency of their single incorporation into a peptide backbone. As was discussed earlier, Merryman and Green performed a similar experiment with a dipeptide synthesis format (Merryman and Green, 2004). In contrast, we here incorporated ^{Me}aa into a 12-mer model peptide, thus involving the incorporation of ^{Me}aa into a specific site followed by elongation and termination of peptide synthesis as a format of normal peptide synthesis (Figure 2A, more details are discussed below).

For this study, we chose 23 ^{Me}aa substrates, 19 of which were derived from proteinogenic amino acids, and 4 of which were derived from nonproteinogenic amino acids (Figure S1, see the Supplemental Data available with this article online). The flexizyme-catalyzed aminoacylation efficiency for each ^{Me}aa was verified by our standard protocol (Figure S2), showing that the majority of ^{Me}aa could be charged onto tRNA with over 30% yields. Three amino acids, ^{Me}Val, ^{Me}Ile, and ^{Me}Asn, showed less than 30% yields. In the former two amino acids, their steric hindrance resulted from the combination of the β-branched side chain and the *N*$^{\alpha}$-methyl-amino group presumably made these particular substrates much less reactive to flexizyme compared with other ^{Me}aa. In the case of ^{Me}Asn, based on our past experience working on Asn-tRNA, its tRNA-adduct might be labile due to the intramolecular attack of the amide side chain (Lee and Suga, 2001; Murakami et al., 2006); thereby the yield might appear to be low in PAGE analysis. However, we have previously observed that such aa-tRNAs prepared in similar ranges of quality (Val-, Ile-, and Asn-tRNAs in 13%–30% yield) could still be used for the incorporation into the nascent peptide chain with satisfactory yields (30%–70%) (Murakami et al., 2006). Thus, we pursued to survey all ^{Me}aa-tRNAs for the single incorporation into the model peptide.

The *w*PURE system used in our survey was composed of a limited member of amino acids and aaRSs. We designed an open-reading frame (ORF) in mRNA (Figure 2A) that expresses a short peptide consisting of fMet-Arg-^{Me}aa-Arg followed by a Flag peptide (DYKDDDDK; D, Asp; Y, Tyr; K, Lys). We selected a Thr codon (ACC) to assign ^{Me}aa and an orthogonal tRNA$^{Asn\text{-}E1}_{GGU}$ (Ohta et al., 2007) for its suppression. When the model peptide was expressed in the presence of uncharged tRNA$^{Asn\text{-}E1}_{GGU}$ in *w*PURE system, no product band appeared on tricine-SDS-PAGE (Figure 2B, lane 2), suggesting that tRNA$^{Asn\text{-}E1}_{GGU}$ could act as an orthogonal tRNA inert against the endogenous aaRSs added to the *w*PURE system.

We next tested the single incorporation of ^{Me}aa charged onto tRNA$^{Asn\text{-}E1}_{GGU}$ into the model peptide sequence. Eight out of 19 ^{Me}aa derived from proteinogenic amino acids were incorporated into the peptide with more than 30% efficiencies relative to wild-type expression (Figure 2B, lanes 1 versus those highlighted in cyan). The incorporation of the designated ^{Me}aa was also confirmed by MALDI-TOF analysis, giving the expected molecular mass as a sole peak in all cases (Figure 2C). Moreover, ^{Me}Thr, ^{Me}Gln, and ^{Me}Trp were modestly incorporated yet gave the single desired product (Figures 2B and 2C, those highlighted in orange). We called these ^{Me}aa molecules that could be incorporated into the peptide chain with more than 10% efficiencies as "accessible" ^{Me}aa. Interestingly, all of these "accessible" ^{Me}aa shared similar structural features of their side chains; either aromatic side chains (^{Me}Phe, ^{Me}Tyr, ^{Me}His, and ^{Me}Trp) or non-charged and nonbulky side chains (^{Me}Gly, ^{Me}Ala, ^{Me}Ser, ^{Me}Cys, ^{Me}Met, ^{Me}Thr, and ^{Me}Gln).

It should be noted that our results were mostly consistent with Merryman's observations, with some contradictions (Merryman and Green, 2004). In their experiments, ^{Me}Val, ^{Me}Ile, and ^{Me}Leu were ranked in the "efficient," or what we referred to as the "accessible," ^{Me}aa group. However, our experiments showed that ^{Me}Val, ^{Me}Ile, and ^{Me}Leu were grouped as rather "inaccessible" ^{Me}aa for incorporation (Figure 2B, lanes 5–7). The difference between the in vitro-transcribed tRNA$^{Asn\text{-}E1}$ and the native cognate tRNAs that Merryman et al. used as ^{Me}aa-carriers may have an effect on their incorporation efficiencies (Dale and Uhlenbeck, 2005; LaRiviere et al., 2001). However, it should be noted that in the Merryman's TLC electrophoresis assay, the mobility of these branched aliphatic ^{Me}aa were indistinguishable from that of the cognate natural ones. Therefore, it was not clearly defined if the observed product spot originated from fMet-^{Me}aa or fMet-aa. Because the reductive alkylation of some aa-tRNAs to generate ^{Me}aa-tRNAs possibly left a small amount of unreacted aa-tRNAs as Merryman et al. discussed (Merryman and Green, 2004), it could not be ruled out that such aa-tRNA contamitants competed out ^{Me}aa-tRNAs for incorporation into the nascent

(C) MALDI-TOF-MS spectra of the Flag-purified N-methyl-peptides. The calculated molecular mass (Calcd.) and observed molecular mass (Obsd.) for singly charged species, $[M+H]^{+1}$ are shown in each spectrum. In the spectrum of peptide with ^{Me}Fni, an additional peak (asterisk) was detected since the additional peak corresponds to *N*$^{\alpha}$-methyl-*p*-nitroso-Phe (Calcd. = 1674.72, Obsd. = 1675.45) generated by photodecomposition of NO_2 to NO during the MALDI-TOF-MS analysis (Ho and Chow, 1996).

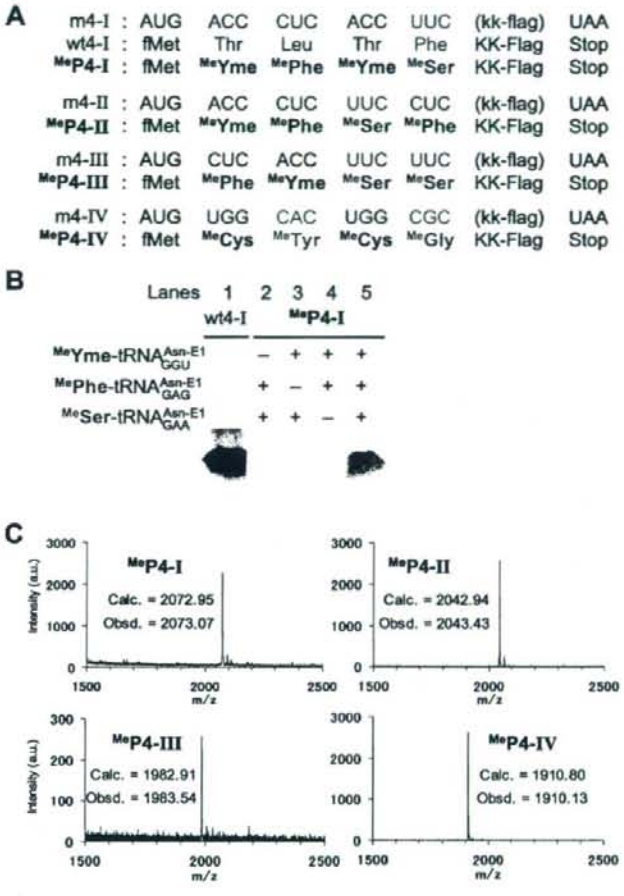

Figure 3. Four Successive Incorporations of Multiple N^{e}-Methylated Amino Acids

(A) Sequences of mRNA templates (m4-I–IV), tetra-N-methyl-peptides (^{Me}P4-I–IV), and the control wild-type peptide (wt4-I). The kk-flag in parentheses indicates the RNA sequence coding a KK-Flag peptide (KKDYKDDDDK). Arabic number denotes the number of N-methylated peptide bonds. The codons and amino acids are colored according to the reprogrammed genetic code table in Figure 1C.

(B) Tricine-SDS-PAGE analysis of the peptides expressed from m4-I labeled with [^{14}C]-Asp detected by autoradiography. Lane 1, the wild-type peptide expressed in the ordinary PURE system; lanes 2–4, negative controls in the presence of two of ^{Me}aa-tRNA^{Asn-E1} as shown; lane 5, in the presence of all three ^{Me}aa-tRNA^{Asn-E1}.

(C) MALDI-TOF-MS spectra of ^{Me}P4-I–IV. The calculated mass (Calcd.) and observed mass (Obsd.) are shown in each spectrum.

peptide chain. In contrast, in our studies, because the flexizyme system ensures the purity of each ^{Me}aa-tRNA, i.e., no contamination of aa-tRNA as confirmed by MALDI-TOF analysis (Figure 2C), we are able to avoid such issues and judge its intrinsic incorporation efficiency more reliably and quantitatively. To this end, we propose that ^{Me}Val, ^{Me}Ile, and ^{Me}Leu are inaccessible substrates due to the combination of bulkiness in the branched side chain and the N^{e}-methylated α-amino group.

Four ^{Me}aa derived from nonproteinogenic amino acids (Figure S1) were also incorporated into the corresponding peptide chain (Figure 2B, lanes 21–25), each of which the MALDI-TOF data was consistent with the expected molecular mass (Figure 2C). Again, the same trend for the incorporation efficiency seemed to apply to these nonproteinogenic ^{Me}aa, where the aromatic ones were incorporated more efficiently than the aliphatic ones. All data taken together, we concluded that ^{Me}aa having "aromatic" or "nonbulky and noncharged" side chains were preferable for the incorporation into the peptide backbone. This information is invaluable for us to select appropriate ^{Me}aa and design specific compositions of N-methylated peptides or peptide libraries while avoiding the risk of potential failure in the synthesis.

Four Successive Incorporations of Multiple N^{e}-Methylated Amino Acids

We next attempted the consecutive incorporations of multiple ^{Me}aa into the peptide backbone via genetic code reprogramming. Five ^{Me}aa derived from proteinogenic amino acids (^{Me}Ser, ^{Me}Phe, ^{Me}Tyr, ^{Me}Cys, ^{Me}Gly) and one derived from a nonproteinogenic amino acid (^{Me}Yme) were selected and assigned arbitrarily to six codons as shown in Figure 1C. The flexizyme system was utilized to charge the respective ^{Me}aa on tRNA^{Asn-E1} bearing the anticodon that reads the assigned codon. We also designed four mRNA templates containing ORFs (Figure 3A, m4-I–IV) that express the corresponding peptides comprised of three different ^{Me}aa in four successive residues (Figure 3A, ^{Me}P4-I–IV). The C terminus of the respective peptides was also designed to contain a modified Flag sequence (KK-Flag = KKDYKDDDDK; D, Asp; Y, Tyr; K, Lys) to facilitate its isolation as well as ionization upon MALDI-TOF analysis.

We first used m4-I to monitor the expression level of ^{Me}P4-I by tricine-SDS-PAGE with a series of appropriate controls (Figure 3B). ^{Me}P4-I was expressed only when all designated ^{Me}aa-tRNA^{Asn-E1}s were present in the *w*PURE system (lanes 2–5), suggesting that no competing background expression of undesignated peptides occurred. The expression level of ^{Me}P4-I was an approximately 20% relative to that of wild-type (wt4-I) expressed in the ordinary PURE system (lanes 1 versus 5). Despite the modest expression level of ^{Me}P4-I, MALDI-TOF analysis of the Flag-purified ^{Me}P4-I gave a single peak with the expected molecular mass, indicating that the assigned codons on mRNA were

correctly read by these ^{Me}aa-tRNA$^{Asn\text{-}E1}$s and the designated tetra-N-methyl-peptide was expressed.

Likewise, ^{Me}P4-II–IV peptides were expressed at levels approximately 15%–20% of the corresponding wild-type peptides (data not shown). Again, MALDI-TOF data of ^{Me}P4-II–IV peptides were consistent with the expected mass (Figure 3C). Thus, all mRNA ORFs tested in this study could be correctly translated to the tetra-N-methyl-peptides according to the assigned codons with high fidelities. This study represents, to our knowledge, the first proof-of-concept experiment for the ribosomal synthesis of N-methyl-peptides containing multiple kinds of ^{Me}aa by the genetic code reprogramming.

Expression of Longer N-Methyl-Peptides

The achieved high fidelity control in the ribosomal synthesis of the tetra-N-methyl-peptides encouraged us to attempt the expression of longer N-methyl-peptides. We designed four mRNA templates that express N-methyl-peptides containing five, six, eight, or ten consecutive N-methyl-peptide bonds (Figure 4A) (m5/^{Me}P5, m6/^{Me}P6, m8/^{Me}P8, m10/^{Me}P10, respectively). These peptides consisted of three ^{Me}aa in a repetition of the sequence ^{Me}Yme, ^{Me}Phe, and ^{Me}Ser for the corresponding length. To compare the expression level of these N-methyl-peptides, the respective wild-type peptides (wt5–10) were also expressed by using the ordinary PURE system.

All mRNA templates successfully expressed the peptides in the presence of the corresponding ^{Me}aa-tRNA$^{Asn\text{-}E1}$s in *w*PURE system (Figure 4B, gel figure). The absolute expression level for each N-methyl-peptide, determined by its radioisotope intensity originating from the incorporation of five [^{14}C]-Asp residues in the Flag peptide, gradually decreased with increasing peptide length (Figure 4B, upper graph). However, since wild-type also exhibited an inverse-correlation between expression level and peptide length, the relative expression levels of N-methyl-peptides to the corresponding wild-types remained in a similar range (10%–20%), suggesting that the relative expression level was independent of length (Figure 4B, lower graph). Despite their modest yields, the respective N-methyl-peptide had a single peak with the expected molecular mass in MALDI-TOF analysis, indicating that all peptides were expressed with high fidelities according to the corresponding mRNA templates assigned with the reprogrammed genetic code (Figure 4C).

In conclusion, our work has clearly demonstrated up to ten successive incorporations of ^{Me}aa into the peptide backbone via genetic code reprogramming with high fidelity control of both the peptide sequence and length. This technology offers a new means for the sequence-controlled synthesis of peptides containing multiple N-methyl-modifications on their backbone.

Synthesis of Cyclic N-Methylated Peptides Closed by a Thioether Bond

With the above method in our hands, we next applied it to the synthesis of cyclic peptides closed by a physiologically stable thioether bond. The foundation of this peptide ring-closing method has been established during the course of our studies on initiation reprogramming (Goto et al., 2008). Briefly, we prepared a *w*PURE system where Met was depleted so that the initiation codon became vacant. This vacant initiation codon was then filled with initiator tRNA$^{fMet}_{CUA}$ charged with an arbitrarily chosen proteinogenic or nonproteinogenic amino acid by the flexizyme system, so that the translation starts from this newly assigned initiator amino acid. When *N*$^{\alpha}$-(α-chloroacetyl)-amino acid (*N*$^{\alpha}$-ClAc-aa) and Cys were assigned to the initiation and elongation codons, respectively, the expressed full-length linear peptide spontaneously cyclized via an intramolecular nucleophilic attack of the sulfhydryl group of the Cys side chain to the N-terminal α-carbon of ClAc group, resulting in the formation of a thioether bond. This technology has enabled us to synthesize various cyclic peptides with any sequences and ring sizes. We here attempted to combine initiation reprogramming with elongation reprogramming using ^{Me}aa, to enable us to devise a flexible and reliable methodology for the mRNA-programmed synthesis of cyclic N-methyl-peptides.

We designed three mRNA templates that express peptides containing multiple N-methylated peptide bonds (Figure 5A, mc-I–III). Six ^{Me}aa (^{Me}Ala, ^{Me}Yme, ^{Me}Tyr, ^{Me}Gly, ^{Me}Ser, ^{Me}Phe) and six proteinogenic amino acids (Phe, Lys, Tyr, Pro, Asp, Cys) were chosen as the components of the cyclic N-methyl-peptides in this study (Figures 5A and 5B, ^{Me}cP-I–III). The respective peptides ^{Me}cP-I–III have two, three, and four N-methylated peptide bonds, respectively, implanted by the newly assigned ^{Me}aa in the codon table shown in Figure 1C. It should also be noted that ^{Me}cP-I and ^{Me}cP-II contain Pro as a proteinogenic component that also gives an additional secondary amide bond. These peptides were expressed in the presence of initiator tRNA$^{fMet}_{CAU}$ charged with *N*$^{\alpha}$-ClAc-Phe and the corresponding ^{Me}aa-tRNAs in the above *w*PURE system. The MALDI-TOF analysis of the Flag-purified ^{Me}cP-I–III showed that all peptides were spontaneously cyclized via a thioether bond upon completion of translation, giving only the programmed cyclic N-methyl-peptides (Figure 5C). This study indicates that this technology is applicable to a wide array of cyclic peptides with multiple N-methyl-peptide bonds.

DISCUSSION

In the first stage of our proof-of-concept studies, we evaluated 19 ^{Me}aa derived from proteinogenic amino acids and 4 ^{Me}aa derived from nonproteinogenic amino acids, to determine the accessible ^{Me}aa. This study has revealed that the ribosome is accessible to ^{Me}aa with aromatic or nonbulky and noncharged side chains for the incorporation into the growing peptide. Most likely the *N*$^{\alpha}$-methyl group added a steric bulkiness to the already bulky structure of certain amino acids, thereby reducing their incorporation levels. It is not yet clear what is the most important filter for the selection of accessible or inaccessible ^{Me}aa, but either EF-Tu or ribosome (or possibly both) is very likely the determinant(s) for their selection (Dale and Uhlenbeck, 2005). Therefore, it is of importance in future experiments to define the selection filter and engineer it to increase the tolerance toward inaccessible ^{Me}aa (Dedkova et al., 2003, 2006).

In this study, we depleted both aaRSs and cognate amino acids from the translation components in order to create vacant codon boxes for ^{Me}aa assignments. In previous studies, the genetic code reprogramming for nonproteinogenic amino acids bearing nonstandard side chains could be achieved by using a PURE system in which only proteinogenic amino acids, not aaRSs, were withdrawn (Murakami et al., 2006). We found,